# CAPILLARY PRESSURE CORRELATIONS FOR UNIFORMLY WETTED POROUS MEDIA

**N.R. MORROW**

***this article begins on the next page*** ☞

JCPT76-04-05

APPLIED RESEARCH

# Capillary Pressure Correlations For Uniformly Wetted Porous Media

Norman R. Morrow,
Petroleum Recovery Institute,
Calgary, Alberta

## Abstract

*The dependence of capillary pressure on wettability as defined by contact angle has been investigated. Drainage and imbibition capillary pressure measurements are presented for six different types of polytetrafluoroethylene (PTFE) porous media. Changes in capillary displacement curvature are shown to be reasonably consistent from one medium to another. The form of these results suggests that operative contact angles which cannot be measured directly within porous media are in reasonable correspondence with contact angles measured at roughened surfaces. To a fair approximation, changes in drainage and imbibition displacement curvatures with contact angle are respectively proportional to the cosines of receding and advancing contact angles observed at rough surfaces. General correlations of the results have been developed.*

*Conditions for observation of spontaneous imbibition behaviour, as predicted by these correlations, are used as a basis for classifying systems as wetted, intermediately-wet or non-wetted. Discussion is given of some aspects of the role of wettability in obtaining improved oil recovery.*

## Introduction

INCENTIVES for the study of wettability in regard to economic methods of obtaining improved recovery of oil from reservoir rocks have been discussed previously[1]. In the only extensive investigation of reservoir wetting behaviour yet reported, advancing contact-angle measurements showed that a wide range of wetting conditions may be encountered from one reservoir to another[2]. Contact angles were measured for reservoir fluids at formation temperatures on minerals which, from examination of thin sections of core samples, were judged to be predominant at the pore walls. It was found that wettability, as determined by contact-angle measurements at smooth surfaces, was qualitatively consistent with relative permeability behaviour. The distribution of wettabilities for the 55 reservoirs for which advancing contact angles were reported is presented as a histogram in Figure 1. Although these results may not be typical of reservoirs in general, they present a distinct contrast to the view that most reservoirs are preferentially water-wet.

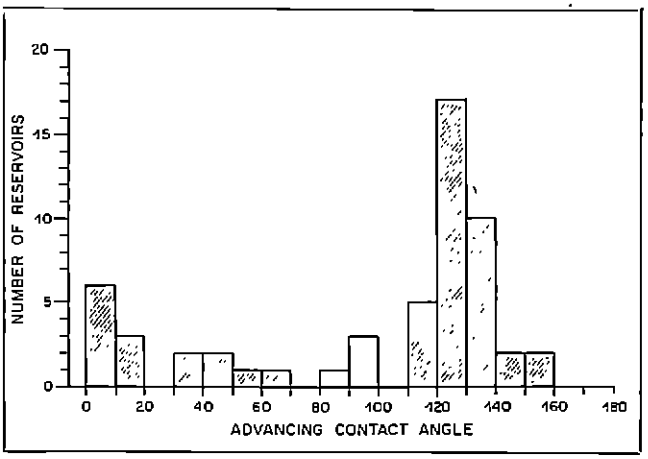


FIGURE 1 — Wettability distribution given by contact-angle measurements on smooth mineral surfaces for fluids from 55 reservoirs.

In practice, when wettability is considered to be important, laboratory data are obtained for preserved cores and fluids at conditions considered to satisfactorily simulate those in the given reservoir. Such data cannot be readily reproduced from one laboratory to another and are difficult to interrelate or quantify. Systematic study under controlled wettability conditions is needed in order to develop an understanding of the role of wettability in oil recovery and other displacement phenomena. Investigations were therefore undertaken of the effects of wettability on spontaneous imbibition[3], capillary pressure and relative permeabilities[4]; a companion study was made to determine the effects of surface roughness on contact angle[5]. A survey of this work has been prepared[6]. The present paper concerns the effects of wettability on relationships between capillary pressure and saturation.

## Background

### Intrinsic Contact Angle

The most reliable method of obtaining precise wettability control in displacement studies is through the use of low-energy solids and pure liquids. Problems which arise in attempting to obtain satisfactory wettability control at high-energy surfaces have been discussed previously[7]. In the present work, PTFE was used as the solid, and the contact angle measured at

**Norman R. Morrow** graduated from the University of Leeds, England, with a B.Sc. (chemical engineering) in 1959 and a Ph.D. (mineral engineering) in 1962. After two years as a research associate in Mineral Engineering at Columbia University, Dr. Morrow entered the petroleum industry. He recently joined the New Mexico Institute of Mining and Technology, where he serves as Head of Basic Studies in the Petroleum Recovery Research Center, and as Adjunct Professor in the Department of Mining and Petroleum Engineering. His main research interests are in surface chemistry and fluid flow in porous media as they relate to enhanced recovery of oil and gas. He is a member of The Petroleum Society of CIM, the Society of Petroleum Engineers of AIME, the American Chemical Society and the Canadian Well Logging Society.

a smooth surface is hereafter referred to as the intrinsic angle, $\theta_E$ (Fig. 2a), which is taken as the basic quantitative measure of system wettability.

## Reference and Non-Reference Phases

Because contact angles at smooth low-energy solids exhibit only very small hysteresis between advancing and receding values[6], the choice of phase through which $\theta_E$ is measured is arbitrary. It follows that a system of wettability $\theta_E$, as measured through one fluid phase, can alternatively be regarded as a system of wettability $(180 - \theta_E)$ with respect to the other phase.

In presenting and discussing results, the intrinsic angle, $\theta_E$, is used to define system wettability, and the fluid through which $\theta_E$ is measured will be termed the reference fluid, and the other fluid the non-reference fluid. When specifying a system and its intrinsic

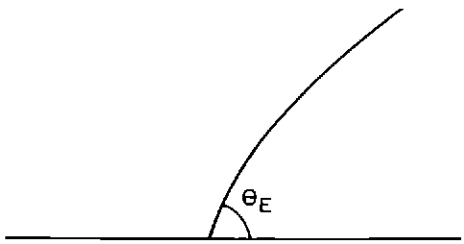


*(a) Intrinsic contact angle.*

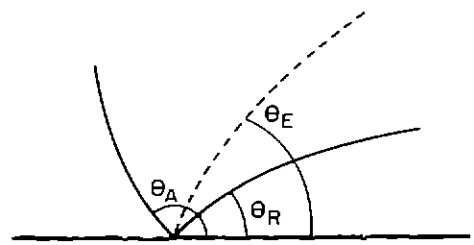


*(b) Contact angle hysteresis at a rough surface*

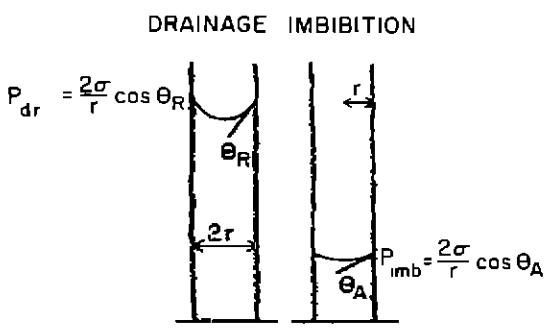


*(c) Hysteresis in capillary rise due to contact angle hysteresis.*

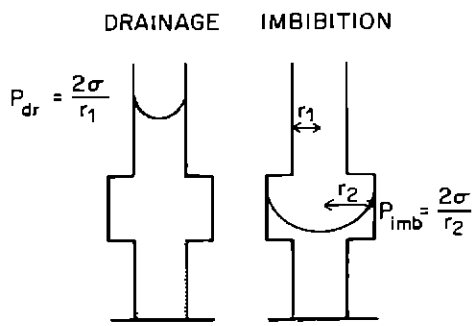


*(d) Hysteresis in capillary rise due to pore geometry.*

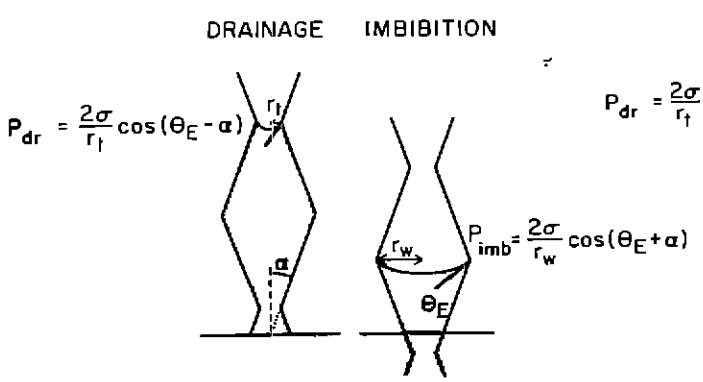


*(e) Hysteresis in capillary rise with interaction of contact angle and pore geometry in absence of contact angle hysteresis.*

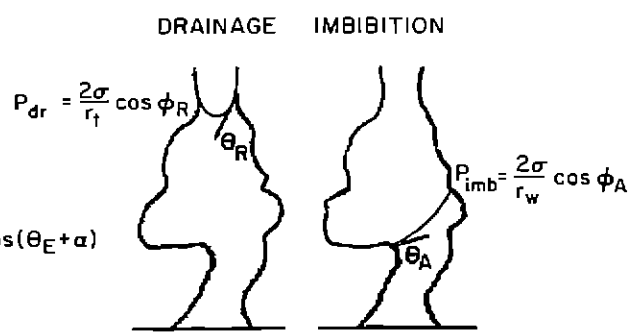


*(f) Hysteresis in capillary rise in an irregular tube with pore geometry and surface roughness effects involved.*

FIGURE 2 — Models illustrating contact angle and capillary pressure phenomena.

angle, the reference fluid is named first. For example, with water and air as fluids the specification would be: either water-air, $\theta_E = 108°$, when water is the reference fluid, or air-water, $\theta_E = 72°$, when air is the reference fluid.

## Effect of Surface Roughness on Contact Angle

In general, surface roughness gives rise to contact-angle hysteresis with distinctly different angles, $\theta_R$ and $\theta_A$, being given under receding and advancing conditions respectively (Fig. 2b). In a previous study[5], advancing and receding angles were determined over a wide range of intrinsic angles from measurements of capillary rise in internally roughened tubes (Fig. 2c). Values of $\theta_R$ and $\theta_A$ for systems of intrinsic wettability $\theta_E$ are presented in Figure 3. These values are remarkably consistent over a wide range of roughness conditions and are believed to be reasonably representative of operative contact angles in the porous PTFE media which were used in displacement studies.

## Capillary Pressure

Capillary pressure is defined as

$$P_c = P_{nr} - P_r \quad (1)$$

where $P_{nr}$ is the pressure in the non-reference fluid and $P_r$ is the pressure in the reference fluid. Drainage is defined as decrease in the reference phase saturation and imbibition as increase in the non-reference phase saturation. Mean curvature ($cm^{-1}$) is defined by

$$J = \frac{P_c}{\sigma} \quad (2)$$

If the wettability of the system is defined by the complementary angle ($180° - \theta_E$), then the reference and non-reference fluids are interchanged accordingly. The basic definition of $P_c$ remains unchanged. Thus, if the wettability of a system with contact angle of 0 degrees is redefined as a system with contact angle of 180 degrees the capillary pressure changes sign. Experimental data are presented as mean curvature versus liquid saturation, the liquid being taken as the reference phase.

## Capillary Pressure Hysteresis At Zero Contact Angle

Capillary pressure hysteresis can be observed for porous media when the contact angle is zero. Considerable attention has been paid to this phenomena, which is basically due to pore shape and is often described as the ink-bottle effect. A simple pore model which exhibits bistability of the interface position depending on whether the pore drains or imbibes is shown in Figure 2d.

## Interaction of Pore Geometry and Contact Angle

When the contact angle is finite, the manner in which capillary pressure is affected depends on the interaction of contact angle and pore geometry, which together provide boundary conditions for capillary structures developed in the porous medium. To illustrate this point, the positions of the onset of instability corresponding to draining and filling of a tube formed from intersecting cones are shown in Figure 2e. The drainage displacement pressure, $P_{dr}$, is given by

$$P_{dr} = \frac{2\sigma}{r_t} \cos(\theta_E - \alpha) \quad (3)$$

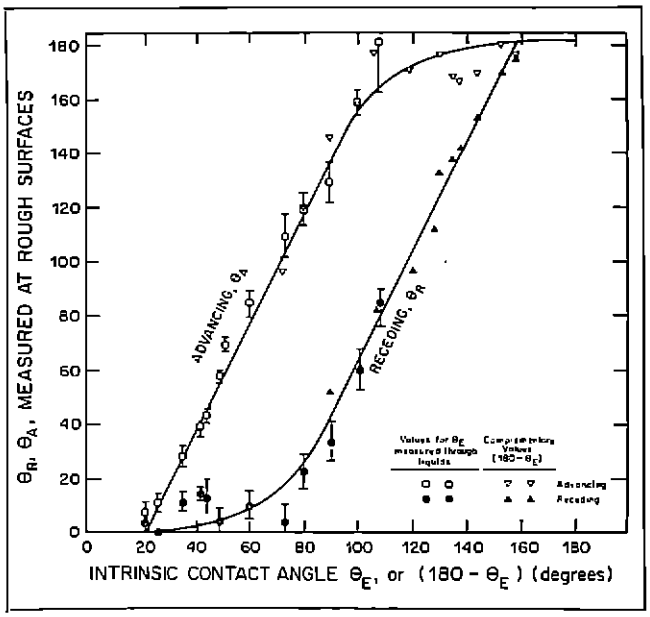


FIGURE 3 — Values of advancing ($\theta_A$) and receding ($\theta_R$) contact angles observed at rough surfaces[5], versus intrinsic contact angle, $\theta_E$.

and the imbibition pressure by

$$P_{imb} = \frac{2\sigma}{r_w} \cos(\theta_E + \alpha) \quad (4)$$

where $\sigma$ is the interfacial tension, $\alpha$ is the half angle of the cone, and $r_t$ and $r_w$ are the radii of pore throat and waist respectively. Physical limitation on the values taken by $(\theta_E - \alpha)$ and $(\theta_E + \alpha)$ are, of course, set by the system geometry. For a system having a rough surface giving receding and advancing contact angles of $\theta_R$ and $\theta_A$ respectively, these equations are modified:

$$P_{dr} = \frac{2\sigma}{r_t} \cos(\theta_R - \alpha) \quad (5)$$

$$P_{imb} = \frac{2\sigma}{r_w} \cos(\theta_A + \alpha) \quad (6)$$

## Apparent Contact Angles for Porous Media

Pores in intergranular porous media are generally beyond detailed mathematical description. By analogy with the equation for capillary rise in a cylindrical tube, apparent contact angles [9] ($\phi_R$ for drainage and $\phi_A$ for imbibition, as illustrated in Fig. 2f) are defined by

$$P_{dr} = \frac{2\sigma}{r_t} \cos\psi_R \quad (7)$$

$$P_{imb} = \frac{2\sigma}{r_w} \cos\phi_A \quad (8)$$

The values of $r_t$ and $r_w$ are those calculated from displacement pressures when the intrinsic contact angle is zero, and $\phi_R$ and $\phi_A$ are set equal to zero.

From the foregoing discussion, it is clear that any general account of the effect of contact angle on displacement requires investigation of the effect of variation in pore geometry from one porous medium to another. To this end, capillary pressure measurements, over a wide range of wettabilities, have been made on six cores having varied physical characteristics.

## Experimental

Artificial cores of consolidated PTFE having porosities ranging from 16.5 to 47.5% were supplied by Allied Nucleonics. The cores were prepared by compacting PTFE powder, of the size distributions listed in Table 1, in steel tubes. The compacted powder was then sintered at 500°F. Radial porosity distribution was determined from weight changes given by machining away concentric annuli from one end of a given core sample. Cores of low porosity, in the range of 16% to 26%, were obtained by applying compression during sintering. The desired effect of producing lower-porosity cores was achieved, but their permeabilities, as measured by Ruska air permeameter, were much lower than expected and too low for use in planned displacement experiments. Properties of the cores chosen for study are listed in Table 2.

TABLE 1 — Size Distribution of PTFE Powder

| Identification | Supplier | Cumulative % Wt. Retained* 32 | 42 | 65 | 80 |
|---|---|---|---|---|---|
| VP 11 | Hoechst | 14.8 | 45.4 | 73.0 | 76.7 |
| VP 16 | Hoechst | 6.9 | 24.0 | 82.4 | 89.2 |
| G 161 | ICI | Powder not available | | | |
| G 2 | ICI | 57.3 | 80.1 | 98.9 | 99.3 |
| G 18 | Allied Chemical | Powder not available | | | |

*U.S. Mesh

Liquids used in the present study are listed with their sources in Table 3. The listed contact-angle values are those given by Fox and Zisman[8]. Observed contact angles at a polished PTFE surface were all in very close agreement with these values.

Detailed studies of the effect of wettability on drainage and imbibition capillary pressure were made on the six core samples listed in Table 2. A range of cores was studied in order to determine the effect of variation in pore geometry from one core to the next. At present, there is no quantitative method of characterising pore geometry. It is assumed that the differences in powder and conditions of consolidation give variation in the geometric structure of pore space. Although four of the cores have porosities in the range of 41.5 ± 1%, variation in structure is indicated by the distinct variation in longitudinal and radial permeabilities from one core to the next.

The apparatus and procedure for measurement of capillary pressure data have been described previously[9]. For consistent results at higher contact angles, it is especially important that the core sample be completely saturated with liquid initially. Cores were first saturated under vacuum, but this did not always give complete saturation. To obtain complete saturation at higher contact angles, as judged from constancy in the volume of liquid held by a given core, additional liquid was forced into the core at pressures of about 1000 psi. From experience gained in the present work, it is recommended that the injection stage of saturating a core be included if a drop of the liquid in

TABLE 2 — Core Properties

| Core Identification Number | Powder | Confining Pressure (psi) | Porosity (per cent) | Permeability (Darcies) Longitudinal | Radial 1 | Radial 2 |
|---|---|---|---|---|---|---|
| 1 | VP 11 | 2000 | 42.5 | 2.6 | 2.8 | 2.9 |
| 2 | VP 16 | 2000 | 47.5 | .32 | 0.013 | 0.020 |
| 3 | VP 11 | 2400 | 41.0 | .2 → 2.0* | * | * |
| 4 | 90% VP11, 10% G161 | 2400 | 36.0 | 1.6 | 0.63 | 0.23 |
| 5 | G 2 | 2200 | 41.0 | 0.7 | 0.045 | 0.053 |
| 6 | G 18 | 1750 | 40.5 | 0.35 | 0.046 | 0.02 |

*Difficulties experienced in measurement because of breakage of cores during mounting.

TABLE 3 — Contact Angles of Liquids Against Air at Smooth PTFE (Teflon) Surfaces

| Liquid | Source of Liquid | Surface Tension (dyne/cm) | Density (g/cc) | Intrinsic Contact Angle ($\theta_E$) (degrees) | Complementary Angles (180 − $\theta_E$) (degrees) |
|---|---|---|---|---|---|
| n-Pentane | Phillips Petroleum Co. (pure grade) | 15.6 | 0.621 | 0 | 180 |
| n-Hexane | Phillips Petroleum Co. | 18.4 | 0.668 | 7 | 173 |
| n-Heptane | Phillips Petroleum Co. | 18.89 | 0.680 | 22 | 158 |
| n-Octane | Phillips Petroleum Co. | 21.22 | 0.699 | 26 | 154 |
| n-Decane | Phillips Petroleum Co. | 23.35 | 0.726 | 35 | 145 |
| n-Dodecane | Phillips Petroleum Co. | 24.9 | 0.743 | 42 | 138 |
| n-Tetradecane | Phillips Petroleum Co. | 26.16 | 0.759 | 44 | 136 |
| Dioctyl Ether | Eastman Kodak Co. | 27.3 | 0.802 | 49 | 131 |
| Hexachlorobutadiene | Eastman Kodak Co. | 36.0 | 1.682 | 60 | 120 |
| α-Bromonaphthalene | Fisher Scientific Co. (reagent grade) | 43.0 | 1.474 | 73 | 107 |
| Ethylene Glycol | Fisher Scientific Co. (certified) | 47.7 | 1.108 | 90 | 90 |
| Water (double distilled) | | 70.6 | 0.977 | 108 | 72 |

question, when placed on the surface of the core, does not imbibe immediately. For the dry cores, it was found that tetradecane ($\theta_E = 44°$) imbibed spontaneously into all cores. Dioctyl ether (49°) was observed to imbibe into core no. 1 only, and hexachlorobutadiene (60°) did not imbibe into any of the cores. Once a core was saturated with any of the liquids listed in Table 3, including water (108°), it could be exposed to the atmosphere without risk of spontaneous drainage of liquid from the core.

Primary drainage curves (from 100% liquid saturation) were measured for pressures, measured in cm of water, of up to 3.6 times the surface tension, $\sigma$, measured in dynes/cm, of the test liquid. This limit was set by the pore size of the semipermeable membrane (nominally 1-2 microns) used in the capillary pressure cell. For those liquids which would spontaneously imbibe, imbibition curves were measured starting from the maximum applied capillary pressure of 3.6 $\sigma$ cm of water.

It was found that there is no measurable effect of contact angle on imbibition or drainage for hexane ($\theta_E = 7°$) or heptane ($\theta_E = 22°$); the results for these systems were equivalent to those for pentane ($\theta_E = 0°$) which spreads on teflon. The use of pentane and hexane involves a number of experimental difficulties and inconveniences, including refrigeration of the apparatus. Results for heptane were therefore assumed to be equivalent to the results which would be given by a completely wetted system. Tests with pentane and hexane on two of the studied cores (nos. 1 and 2) confirmed the validity of this approach.

Attempts were made to measure capillary pressure data for drainage of air by injection of liquids which do not imbibe spontaneously, but these were only partially successful. Core no. 1 was used as the test media and a preferentially air-wet membrane was machined from PTFE media of smaller pore size. Drainage of air from 100% air saturation was measured for both water and $\alpha$-bromonaphthalene. The range of measurement was limited to about 50% desaturation because the cell membrane was penetrated by the liquid at the higher injection pressures.

## Results

Results for cores 1 through 6 are shown in Figures 4 through 9 respectively. In addition, data obtained

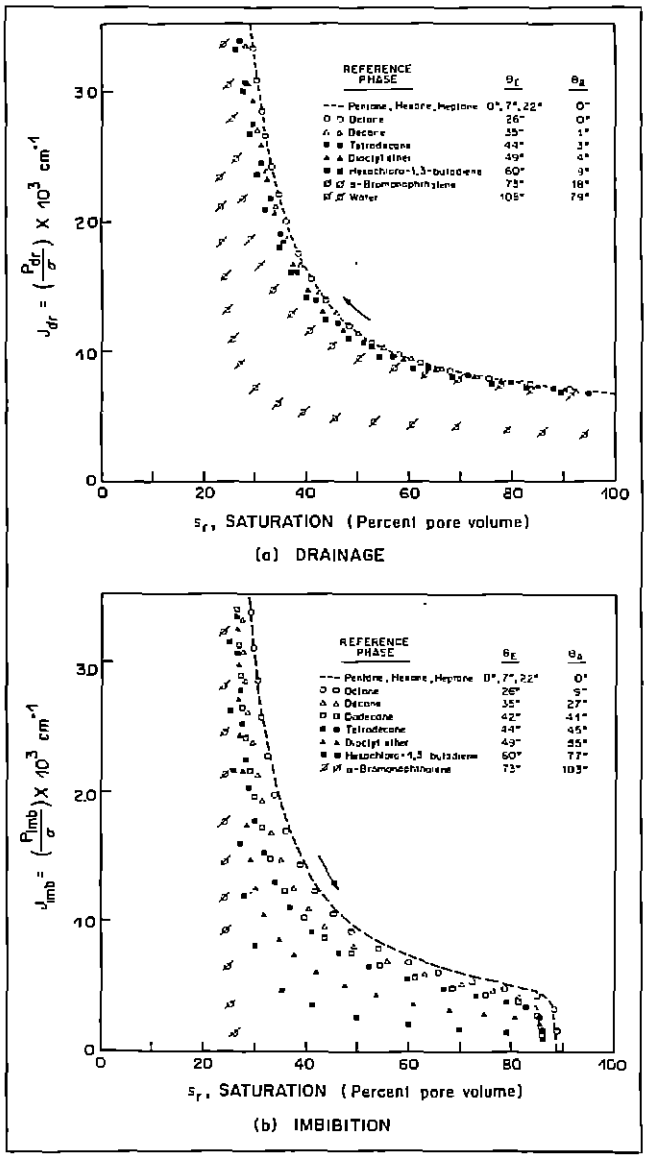


FIGURE 4 — Effect of contact angle on capillary pressure, core No. 1.

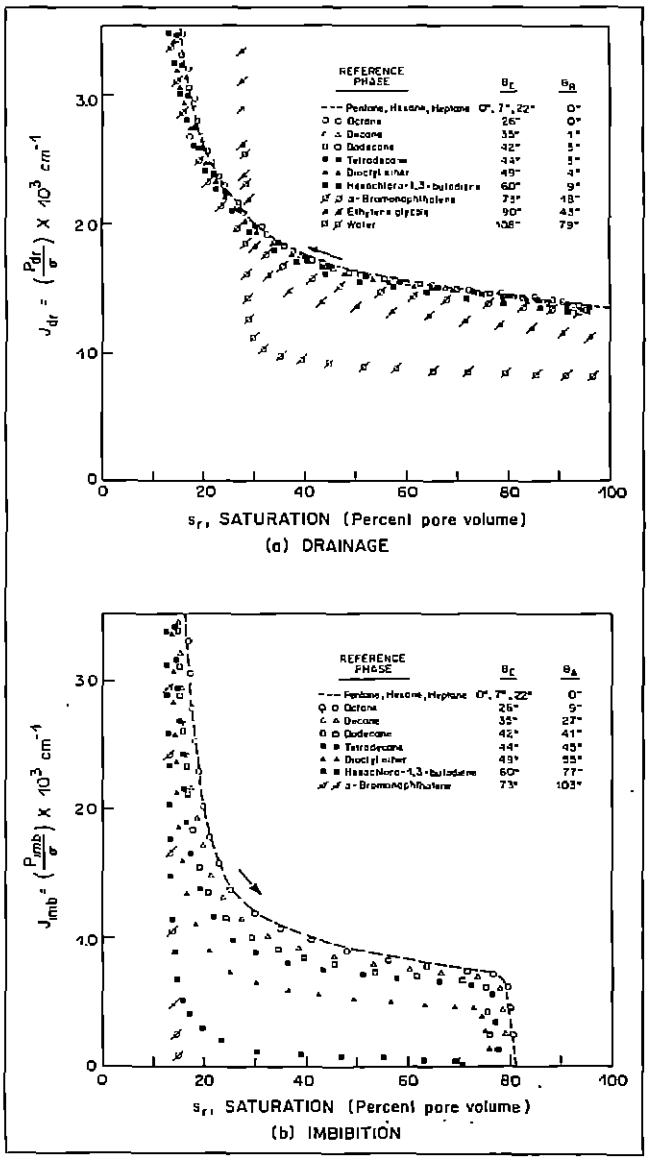


FIGURE 5 — Effect of contact angle on capillary pressure, core No. 2.

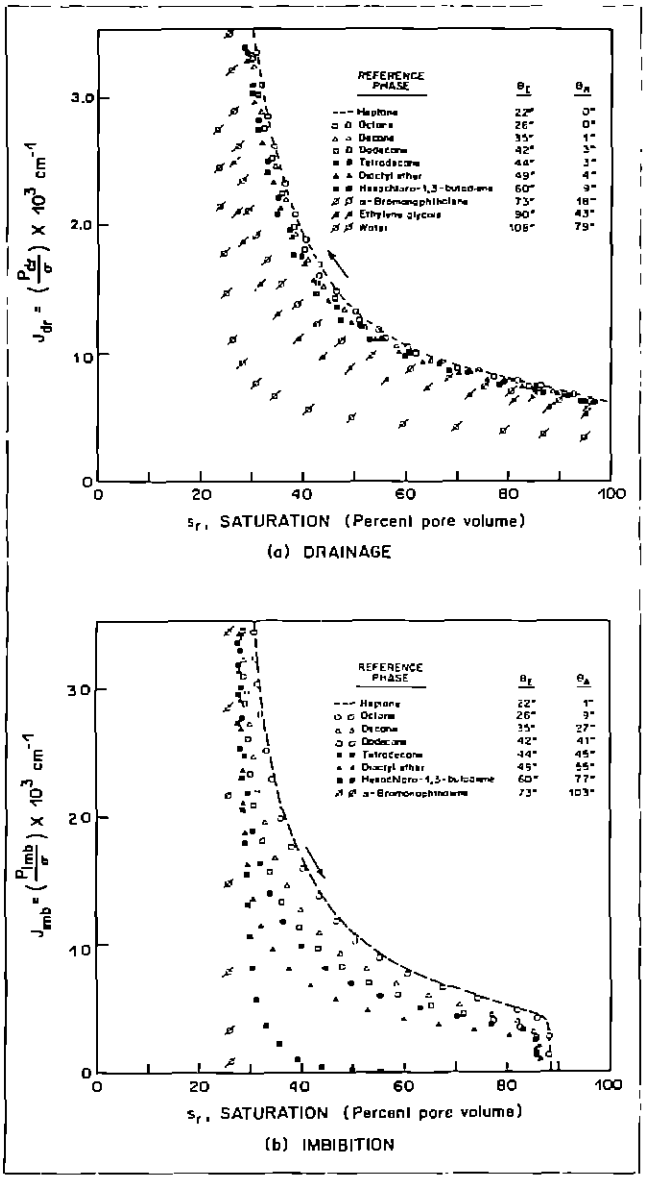


FIGURE 6 — Effect of contact angle on capillary pressure, core No. 3.

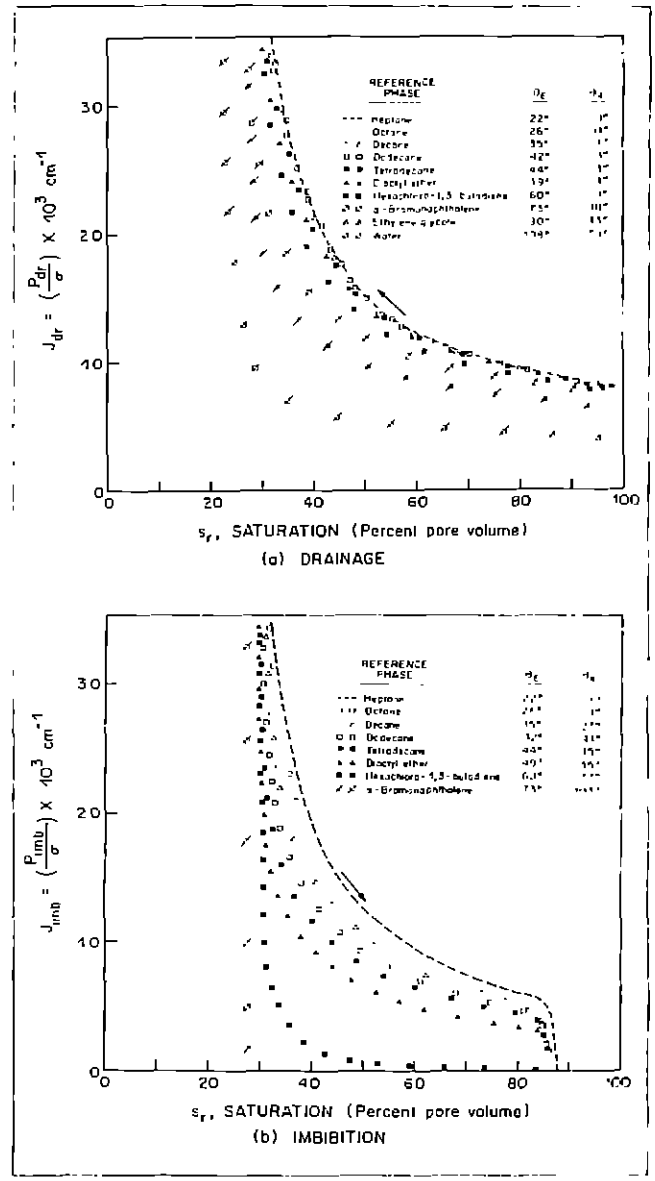


FIGURE 7 — Effect of contact angle on capillary pressure, core No. 4.

for drainage of air from core no. 1 by injection of liquid gave added confidence in the use of intrinsic contact angle as a basic measure of wettability. Results for air-water ($\theta_E = 72°$) were in very close agreement with results shown in Figure 4a for $\alpha$-bromonaphthalene-air ($\theta_E = 73°$). Similarly, results for air-$\alpha$-bromonaphthalene ($\theta_E = 107°$) were essentially the same as those for water-air ($\theta_E = 108°$), which are also given in Figure 4a.

Drainage and imbibition results are presented separately in each case, with intrinsic contact angle as a parameter. Contact angles at rough surfaces, $\theta_R$ for drainage and $\theta_\wedge$ for imbibition, are given in parenthesis. In general, it was found that capillary pressure changed systematically with contact angle and the changes appeared reasonably consistent from one core to the next. Thus, with regard to a main objective of the study, it is concluded that, for the cores studied, the interaction of contact angle and pore geometry is reasonably consistent from one core to another.

A limited study was made of internal scanning curves for core no. 4 for a contact angle of 49 degrees. The curves are shown in Figure 10; numbers indicate the sequence of measurement. Results followed the general laws of behaviour which have been observed for completely wetted systems[10, 11]. One reason for making these measurements was to examine the effect of degree of desaturation on the shape of imbibition curves. This and other features of data presented in Figures 4 through 10 are discussed in more detail in the following development of general correlations of results.

## Correlations

### CORRELATION OF DRAINAGE DATA

#### Normalizing Procedures for Saturations

In order to compare displacement pressures over the complete range of desaturation, for a given core and also from one core to another, some type of procedure for normalizing saturation is needed. For systems which exhibit a distinct irreducible saturation, $s_{ri}$, of the reference phase, saturation $s_r$, an obvious

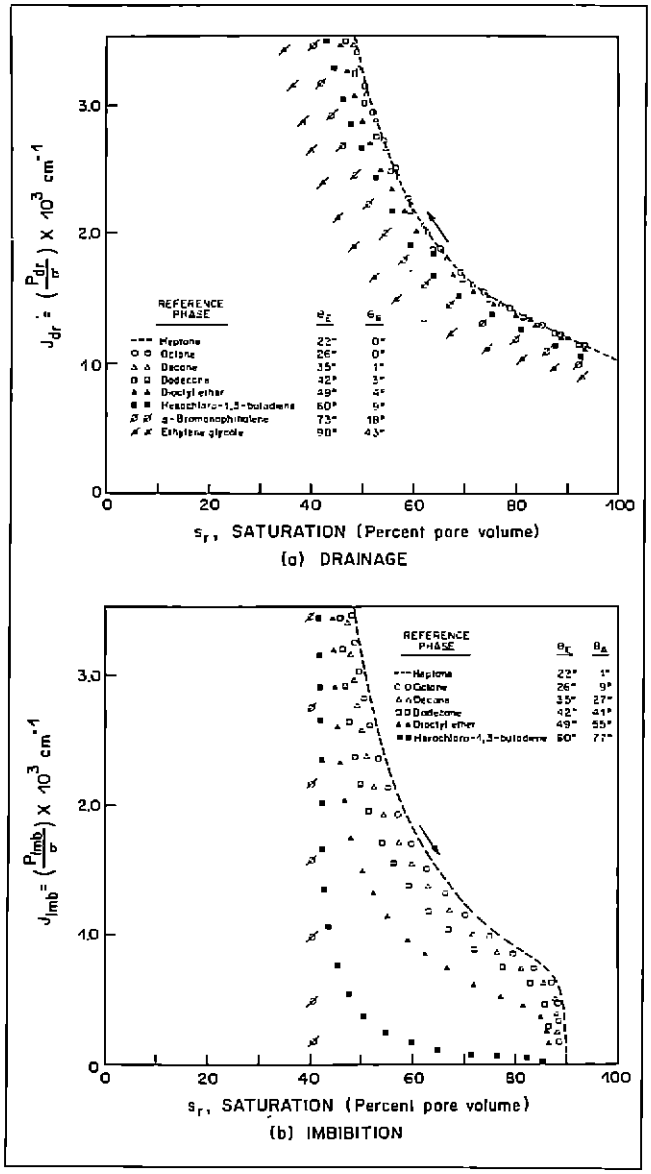


FIGURE 8 — Effect of contact angle on capillary pressure, core No. 5.

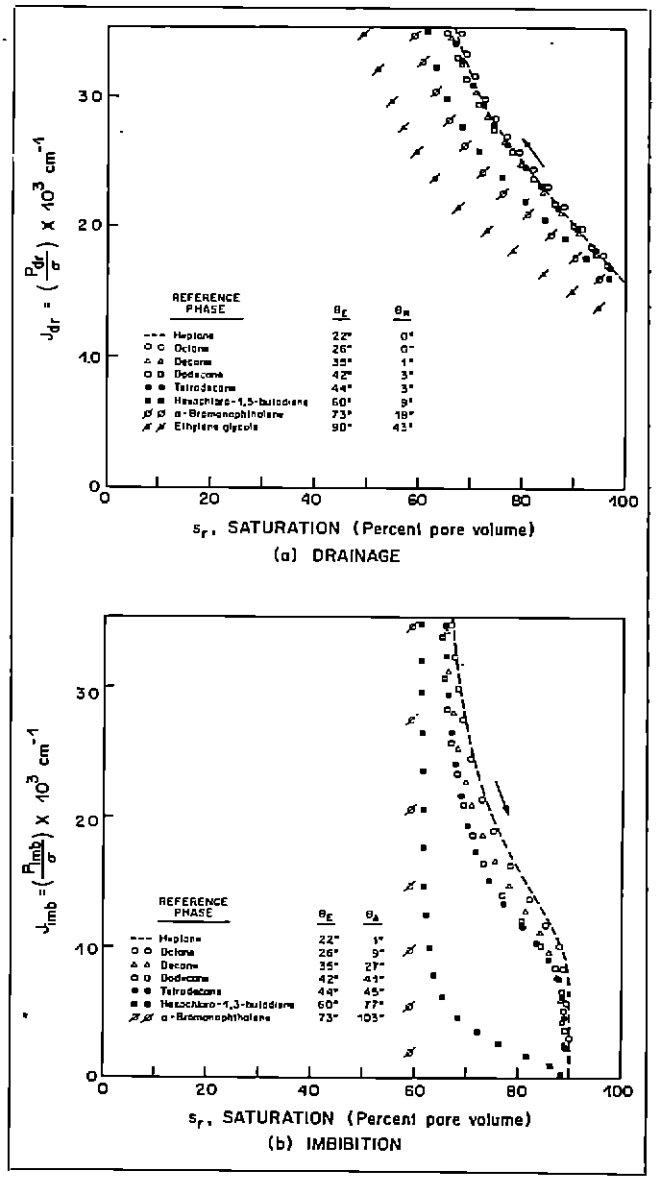


FIGURE 9 — Effect of contact angle on capillary pressure, core No. 6.

choice of normalizing saturation is

$$(s_r)_{NI} = \frac{s_r - s_{ri}}{100 - s_{ri}} \cdot 100 \quad \ldots\ldots\ldots\ldots\ldots\ldots \quad (9)$$

In a previous study of irreducible saturation, a limited study was made of the effect of contact angle[12]. For a random packing of 3-mm PTFE spheres, results fell within ± 1.3% saturation, and the irreducible saturation showed no systematic shift with contact angle over the range of 0 degrees to 108 degrees. In the present work, distinct irreducible saturations were not obtained, but retained liquid saturations showed a systematic decrease with contact angle for all cores except No. 2. Alternative normalizing procedures to that of Equation 9 were therefore tested.

Physically, it is desirable that the saturations for a given core be correlated in a way which permits comparison of the effect of contact angle on displacement on a pore-by-pore basis. However, the saturation at which a given pore drains may vary with contact angle for several possible reasons:

(a) changes in the number of pores in which drainage occurs, resulting in change in the volume of liquid retained in discontinuous form at a given stage of drainage;

(b) apart from the changes in number, there may be changes of sequence for those pores which do participate in drainage;

(c) changes in the volume of capillary structures associated with changes in curvature of bounding interfaces.

It seems likely that change in sequence will be of second-order importance, provided that, as in data reported in the present work, there is no change of sign of capillary pressure of the data being correlated. Of the other two factors, change in the number of pores which drain is considered to be the more important. In the absence of detailed knowledge of the mechanism of drainage, methods of normalizing saturation data were restricted to linear expressions analogous to that defining $(s_r)_{NI}$. The basic problem is then the choice of a normalizing saturation to replace $s_{ri}$ of Equation 9.

Of several approaches which were tested, a previously suggested method[13] of defining a characteristic retained liquid saturation was found to be the

most satisfactory. For each drainage curve, a threshold entry curvature, $J_E$, was defined by extrapolating the plateau of the capillary pressure curve to 100% saturation. Values of $s_r$ given by values of $J_{dr}/J_E$ = 2.5, 3.0 and 3.5 (Fig. 11) were then tested as normalizing saturations. It may be noted that

$$\frac{J_{dr}}{J_E} = \frac{P_{dr}}{P_E} \quad \ldots\ldots \quad (10)$$

where $P_E$ is the entry pressure. The following discussion of these dimensionless ratios will be given in terms of pressure.

The rationale for the above choice of normalizing saturations for the reference fluid was as follows. In general, the entry pressure is a well-defined feature of a drainage curve. The shift in entry pressure with contact angle is related to the effect of contact angle on displacement curvature for the largest pores. If it is assumed that this effect is the same for all sizes of pore, then at a given multiple of the entry pressure, the saturation should in general correspond to the drainage of a given pore. This rationale could be applied over the whole saturation range, but in order to obtain a linear transformation similar to that given by Equation 9 it was pursued no further than defining a normalizing saturation, $(s_r^*)_{N_r}$ of the reference fluid.

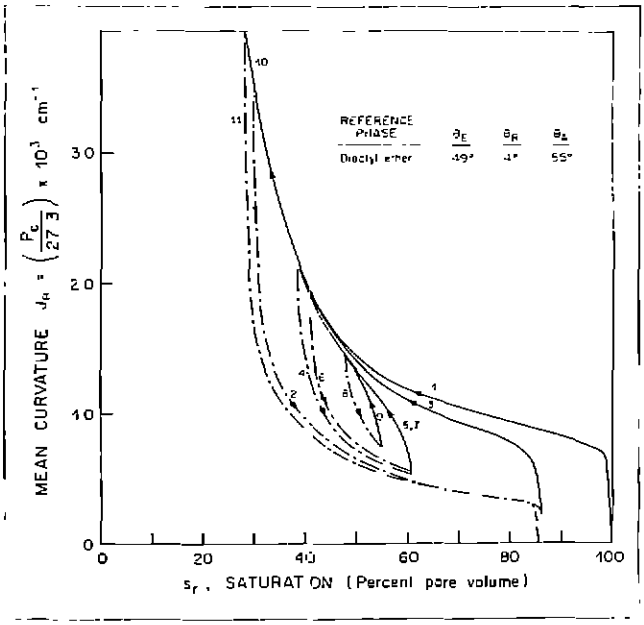


FIGURE 10 — Scanning curves for core No. 4.

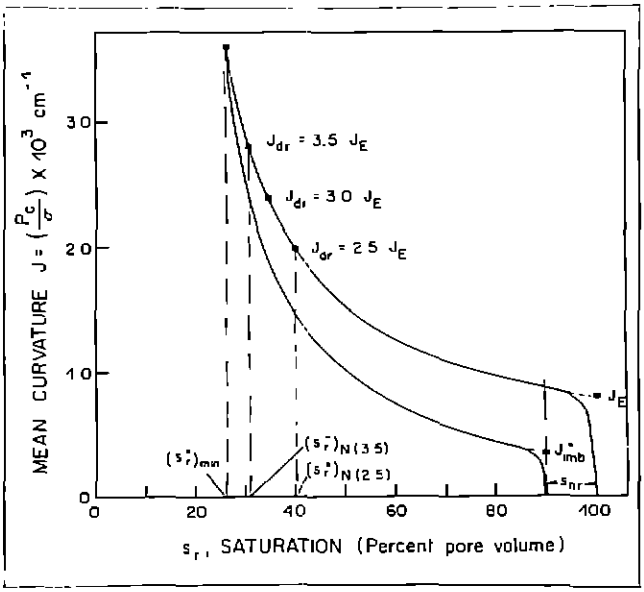


FIGURE 11 — Drainage-imbibition relationships, illustrating method of selecting correlating parameters.

For five of the six cores studied, values of $(s_r^*)_N$ decreased with contact angle. Results for core no. 2 were anomalous in that all $(s_r^*)_N$ values were relatively high for water and ethylene glycol (Fig. 5a). It was not convenient to repeat these measurements. However, loss of hydraulic contact between the core and membrane is suspected as the cause of these results, as these were the only instances in which distinct irreducible saturations were observed. It may also be noted that this apparent loss of hydraulic contact for ethylene glycol and water occurred at the same saturation in each case. In developing a general correlation, results obtained for core no. 2 were excluded; further reference to results for five cores involves cores 1, 3, 4, 5 and 6.

Values of $(s_r^*)_N$ for five cores at $(P_{dr}/P_E)$ ratios of 2.5, 3.0 and 3.5 are shown in Figures 12a, b and c respectively. The normalized saturations, $(s_r)_N$, in the case of $P_{dr}/P_E$ = 2.5 for example, are then given by

$$(s_r)_{N(2.5)} = \frac{s_r - (s_r^*)_{N(2.5)}}{100 - (s_r^*)_{N(2.5)}} \times 100 \quad \ldots\ldots \quad (11)$$

An important development in obtaining a generalized correlation of drainage data arose from normalizing the data shown in Figures 12a, b and c with respect to values of $(s_r^*)_{N,\,\theta=0}$. This gave a generalized relationship:

$$\frac{(s_r^*)_{N,\theta}}{(s_r^*)_{N(\theta=0)}} \text{ vs. } \theta_E$$

shown in Figure 12d, which was fairly insensitive to the ratio $(P_{dr}/P_E)$.

## Effect of Contact Angle on Drainage Curvatures

The effect of contact angle on displacement pressures was expressed in terms of curvature ratio $(J_{dr})_R$:

$$(J_{dr})_R = \frac{(J_{dr})_\theta}{(J_{dr})_{\theta=0}} \quad \ldots\ldots \quad (12)$$

where $(J_{dr})_\theta$ is the drainage curvature, $P_{dr}/\sigma$, at contact angle $\theta$, and $(J_{dr})_{\theta=0}$ is the drainage curvature at zero contact angle. Figure 13a shows the relationship $(J_{dr})_R$ vs $(s_r)_{N(2.5)}$ for contact angles of 73, 90 and 108 degrees. Results shown in Figure 13a and also those obtained for lower contact angles were averaged and smoothed to give the relationships shown in Figure 13b. Similar relationships of

$$\frac{(J_{dr})_\theta}{(J_{dr})_{\theta=0}} \text{ vs } (s_r)_{N(2.5)}$$

are shown in Figure 13c. The smoothed data were replotted as $(J_{dr})_R$ versus intrinsic contact angle with saturation as a parameter (Figs. 14a and 14b). These relationships were used to obtain the interpolated values (for 40° to 90° at 10-degree intervals and 90° to 120° at 5-degree intervals) included in Figures 13b and 13c. Relationships for 115 and 120 degrees, shown as dashed lines, are subject to the obvious uncertainties of the extrapolations to zero curvature ratio shown in Figures 14a and b.

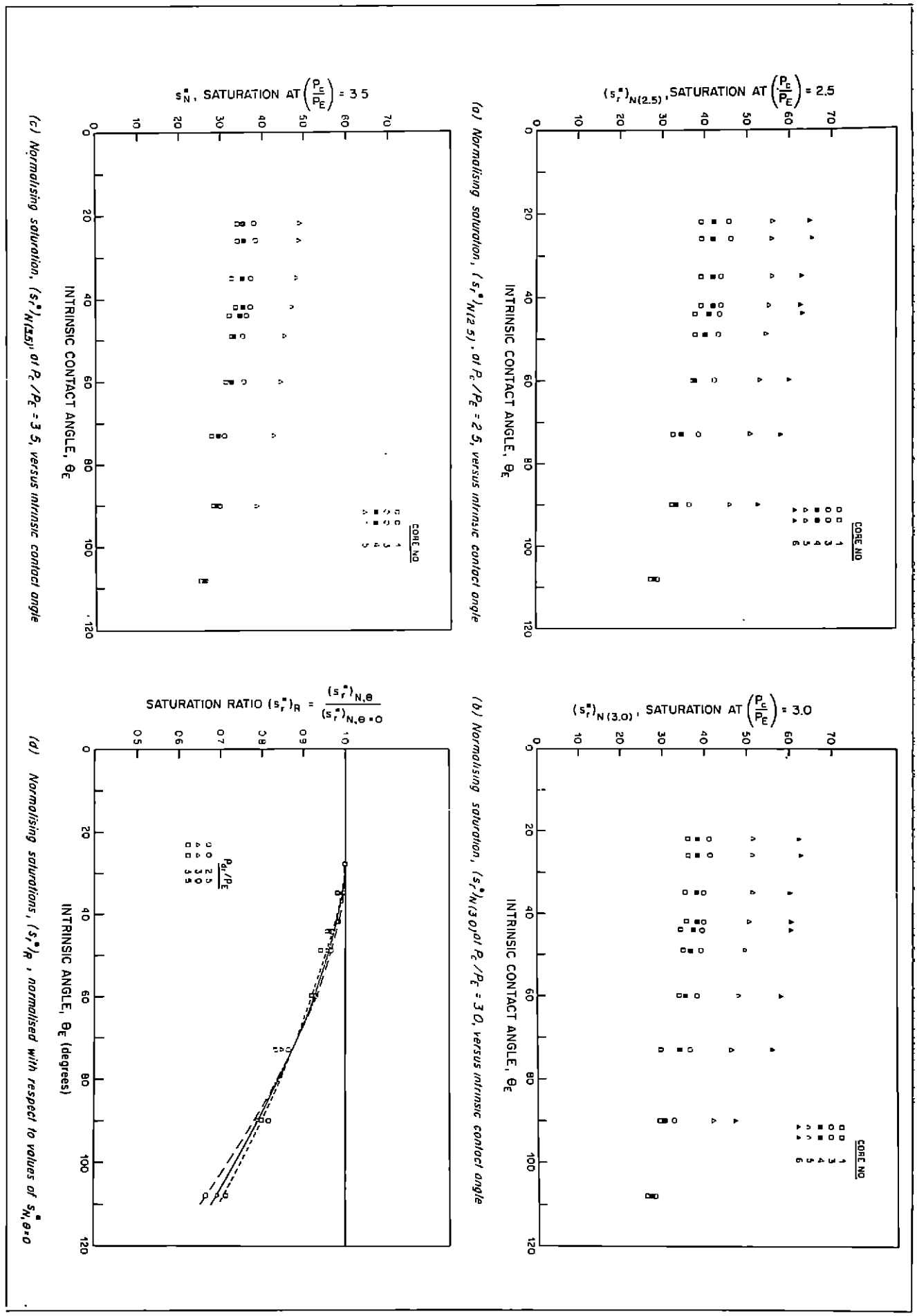


FIGURE 12 — Relationships between retained reference phase saturation and intrinsic contact angle.

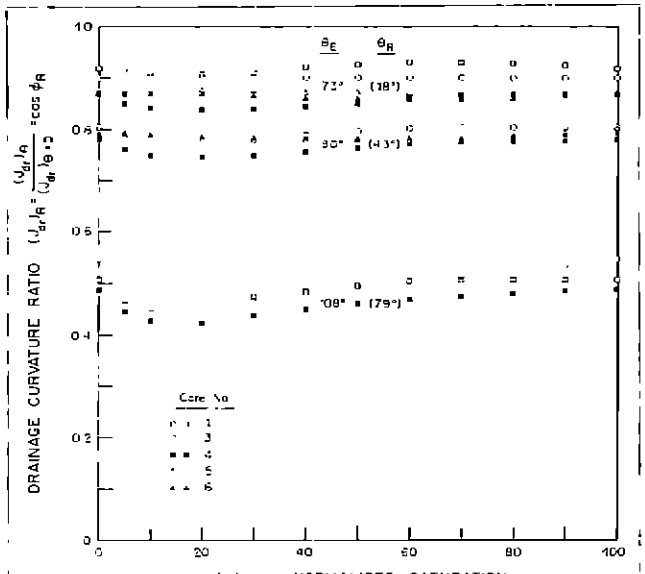


(a) Drainage curvature ratios versus normalised saturation, $(s_r)_{N(2.5)}$

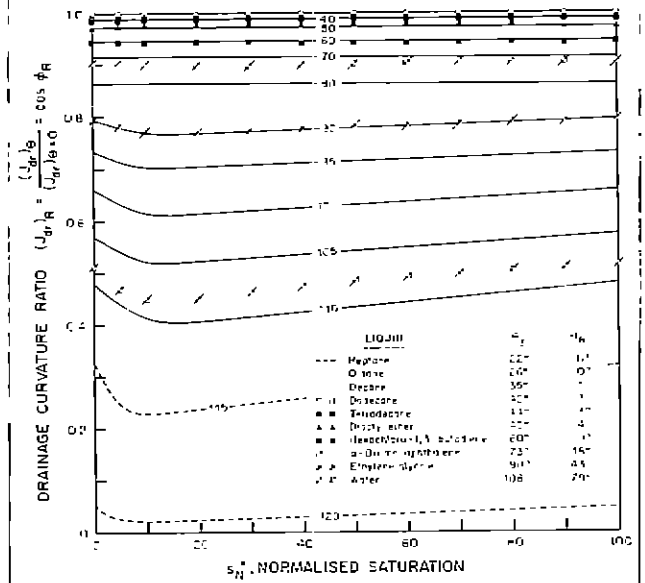


(b) Smoothed and interpolated results for drainage curvature versus normalised saturation $(s_r)_{N(2.5)}$

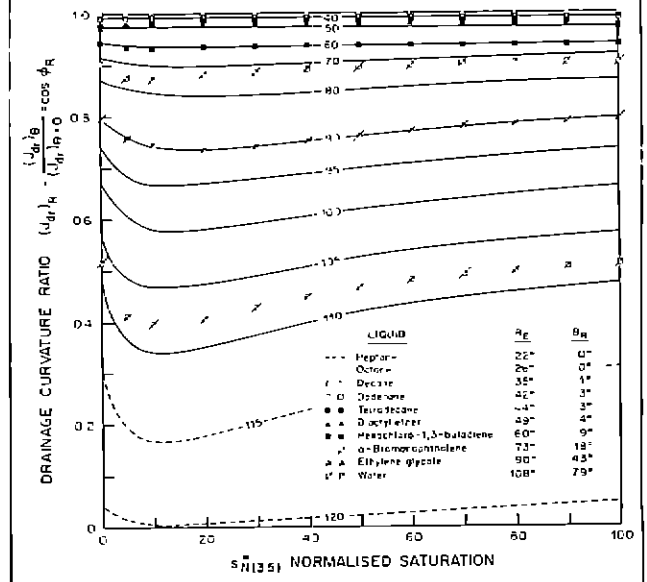


(c) Smoothed and interpolated results for drainage curvature versus normalised saturation $(s_r^*)_{N(3.5)}$

FIGURE 13 (left) — Relationships between drainage curvature and normalized saturation.

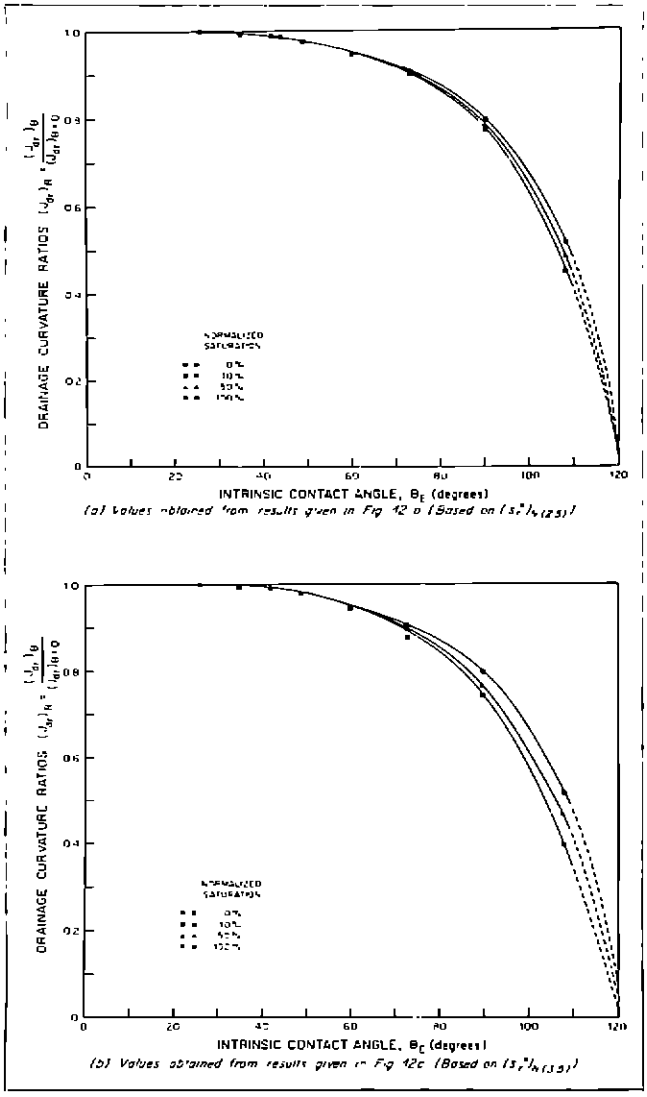


(a) Values obtained from results given in Fig. 12a (Based on $(s_r^*)_{N(2.5)}$)

(b) Values obtained from results given in Fig. 12c (Based on $(s_r^*)_{N(3.5)}$)

FIGURE 14 — Curvature ratio versus intrinsic contact angle for normalized saturations of 0%, 10%, 50% and 100%.

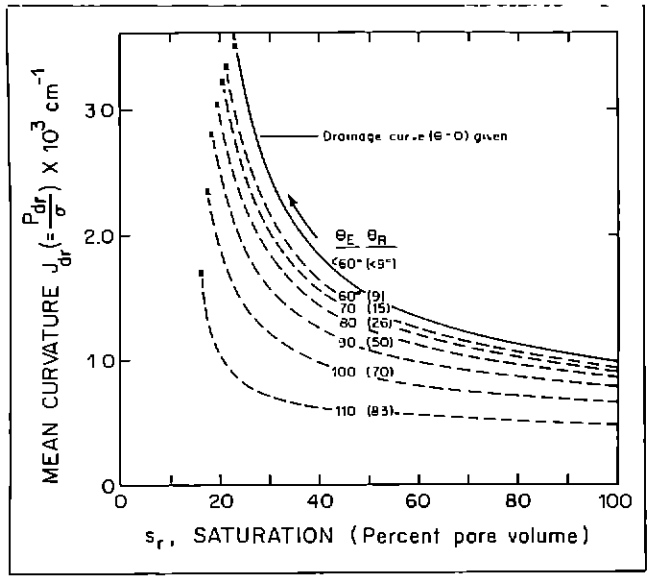


FIGURE 15 — Predicted drainage data for intrinsic contact angles of 60 to 110 degrees at 10-degree intervals.

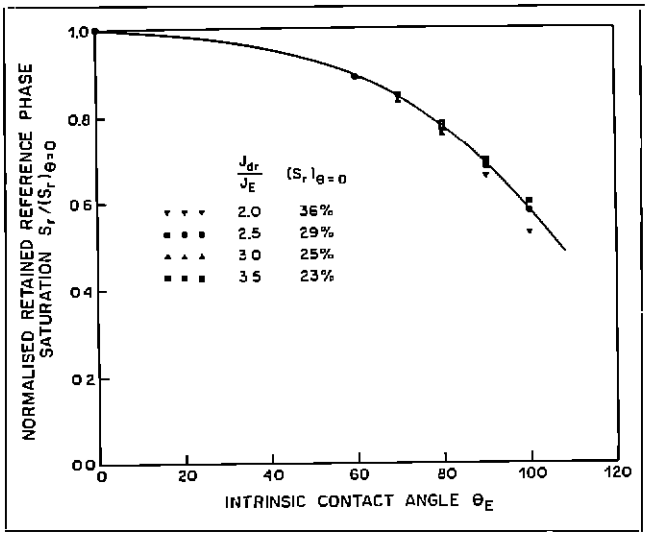


FIGURE 16 — Relationship between retained reference phase saturation and contact angle.

## Prediction of Drainage Data

As an example of the use of the correlated data, consider that results for zero contact angle are given (this wettability condition is one which can usually be reliably established by using gas and oil in core testing), and that drainage curves for intrinsic angles of 60, 70, 80, 90, 100 and 110 degrees are required. From the given curve shown in Figure 15, $(\bar{s}_r^*)_{N(3.5)_{\theta=0}}$ is 23.3 %. From Figure 12d, in the case of $\theta$ = 100 degrees for example, $(\bar{s}_r^*)_{N(3.5)}$ is determined as 0.75 × 23.3% = 17.5%. The zero contact angle data are normalized:

$$(S_r)_{N(3.5)} = \frac{S_r - 23.3}{100 - 23.3} \times 100$$

and Figure 13c is used to obtain the normalized capillary pressure data at the various specified contact angles. In the case of $\theta$ = 100 degrees, for example, actual saturations are then obtained from

$$S_r = (\bar{s}_r^*)_{N(3.5)}\ (1.0 - 0.175) + 17.5$$

to give the curve for 100 degrees included in Figure 15. The same procedure was used to obtain the curves for contact angles of 60, 70, 80, 90 and 110 degrees, which are also included in Figure 15.

## Effect of Contact Angle on Retained Liquid Saturation

It may be noted that because of the procedures used to obtain relationships between saturation ratio $(\bar{s}_r^*)_R$ and $\theta_E$ given in Figure 12d, this correlation does not represent a direct measure of the effect of contact angle on retained liquid saturation at a given displacement curvature. Relationships between retained liquid-saturation $s_r$ and intrinsic contact angle, for the results given in Figure 15, are presented in Figure 16 with relative displacement curvature as a parameter.

# CORRELATION OF IMBIBITION DATA

## Residual Non-Reference Phase Saturations

Correlation of imbibition data involves normalizing saturations for both fluid phases. Residual non-reference phase saturations, $s_{nr}^*$, were determined by straight-line extrapolation of the lower portion of the imbibition curve to zero capillary pressure, as illustrated in Figure 11. Values of residual saturation versus contact angle, presented in Figure 17a, show a tendency for residual saturation to increase with contact angle. Compared with the values of retained reference phase saturation vs. contact angle data shown in Figures 12a, b and c, it is seen that there is considerably more scatter in the residual nonwetting phase saturations. Possible reasons for the scatter are escape of the residual entrapped air by diffusion and the difficulty of defining the residual at low imbibition curvatures. The cause of this scatter could likely be resolved by a study in which specific attention is given to accurate determination of the effect of contact angle on residual saturations.

The proportional change in residual air saturation with intrinsic contact angle relative to the residual saturation at zero contact angle was determined for

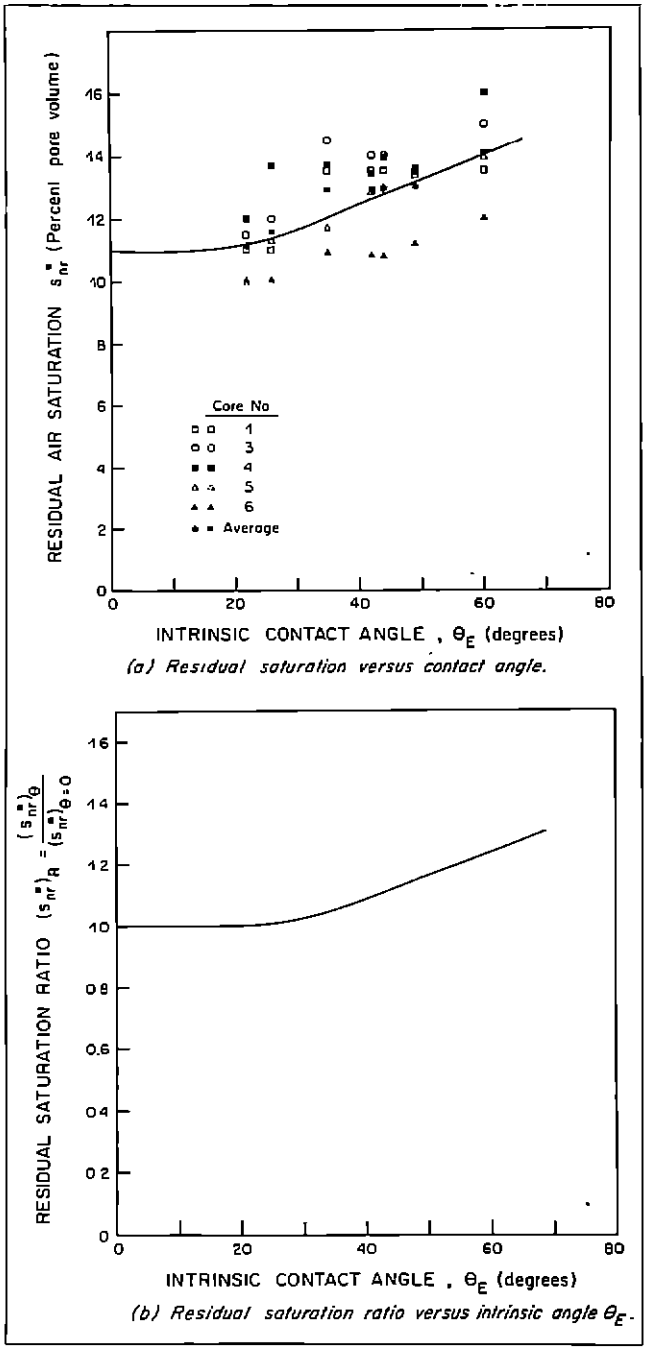


FIGURE 17 — Relationship between residual saturation and intrinsic contact angle.

each core. These values were averaged and smoothed to give the general relationship shown in Figure 17b. Although this correlation is considered reasonably satisfactory for present purposes, it should be noted that it was developed from somewhat scattered data for five cores which all gave relatively low residuals covering only a narrow range of values. Before making assumptions as to the general validity of the relationship given in Figure 17b. it would be desirable to determine the effect of contact angle on residual saturations for porous media exhibiting higher residual saturations (say in the range 15-40%).

## Normalizing Saturations for the Reference Phase

The choice of normalizing saturation for the liquid phase is associated with the more general problem of correlating imbibition data which do not begin at a distinct irreducible saturation. Whereas the primary drainage curve (drainage from 100% reference phase saturation) is unique, it can be seen, from the data shown in Figure 10 for example, that the shape of the imbibition curve depends on the saturation at which measurement is begun. Thus, an additional parameter is needed to characterize the relative position of the imbibition curve with respect to the primary drainage curve.

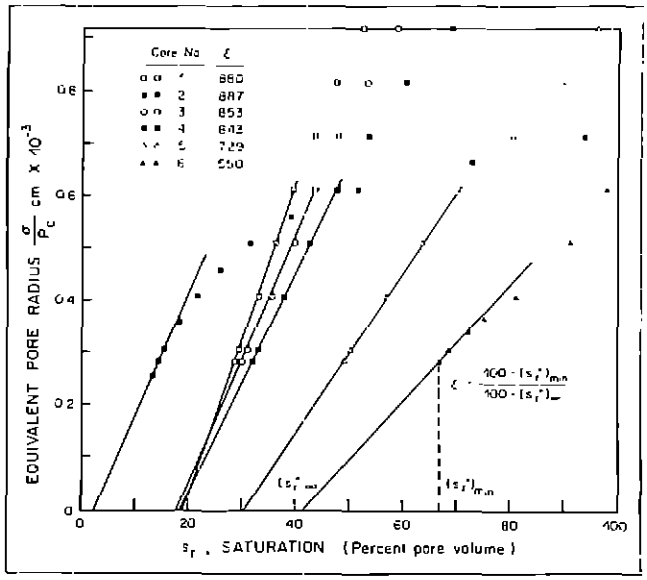


FIGURE 18 — Graphical procedure for determining degree of desaturation, $\xi$.

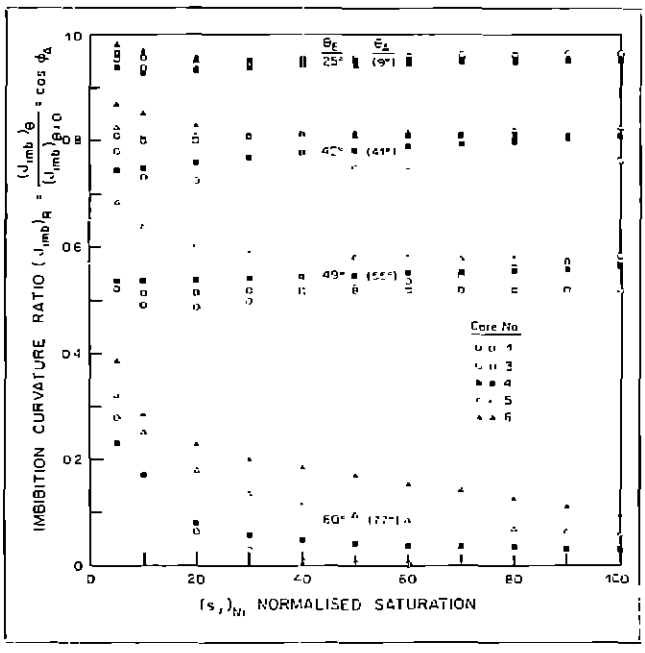


FIGURE 19 — Imbibition curvature versus normalized saturation.

Assuming that the primary drainage curve becomes increasingly steep and approaches some asymptotic value of saturation, it is clear that the significance of the change in shape of the imbibition curve will decrease as this saturation value is approached. A rough guide to the degree of desaturation achieved for a given drainage curve was determined as follows. The drainage data for zero contact angle for each core was replotted as $\sigma/P_{cr}$ versus saturation, as shown in Figure 18. The data were extrapolated (the plots happened to be amenable to straight-line extrapolation) to obtain a saturation $(s_r^*)_\infty$ at infinite curvature. For a core which was drained to a saturation $(s_r^*)_{min}$ before measurement of the imbibition data, the degree of desaturation, $\xi$, was expressed as

$$\xi = \frac{100 - (s_r^*)_{min}}{100 - (s_r^*)_\infty} \quad \ldots \quad \ldots \quad (13)$$

Values of $\xi$ for the six cores which were studied ranged from 0.55 to 0.89 and are listed in Figure 18.

As a general method of predicting capillary pressure results at higher pressures, the extrapolation procedure seems reasonable. However, there is no sound physical basis for its use, and it may be noted that a second inflection in the drainage curve is sometimes obtained for carbonate rocks[14]. A useful feature of the method of plotting used in Figure 18 is that it provides a direct measure of the equivalent radius in cm of the pores in which displacement is taking place.

## Effect of Contact Angle on Imbibition Curvature

The effect of contact angle on imbibition curvatures was expressed in terms of a curvature ratio:

$$(J_{imb})_R = \frac{(J_{imb})_\theta}{(J_{imb})_{\theta=0}} \quad \ldots \quad \ldots \quad \ldots \quad (14)$$

where $(J_{imb})_\theta$ is the curvature at contact angle $\theta$ and $(J_{imb})_{\theta=0}$ is the curvature at contact angle 0 degrees. Normalized saturations for imbibition data were determined from

$$(s_r)_{Ni} = \frac{s_r - (s_r^*)_{min}}{100 - s_{nr}^* - (s_r^*)_{min}} \cdot 100 \quad \ldots \quad \ldots \quad (15)$$

Because the value of $(s_r^*)_{min}$ was determined by the highest capillary pressure reached before measurement of imbibition, its value in terms of the desaturation process is somewhat arbitrary from one core to another. The value of $(s_r^*)_{min}$ is related to the degree of desaturation, $\xi$, through Equation 13.

Plots of curvature versus normalized saturation are shown in Figure 19. The curves for a given contact angle are seen to be reasonably well grouped. There was a tendency, at a given wettability, for imbibition curvatures to decrease as $\xi$ increased. However, in the absence of comprehensive sets of imbibition scanning curves for given contact angles, development of a correlation which attempts to include $\xi$ as a quantitative parameter of imbibition was not considered to be justified. Imbibition results for hexachlorobutadiene for core No. 1 were a notable exception from the general form of behaviour and were excluded in the development of a general correlation.

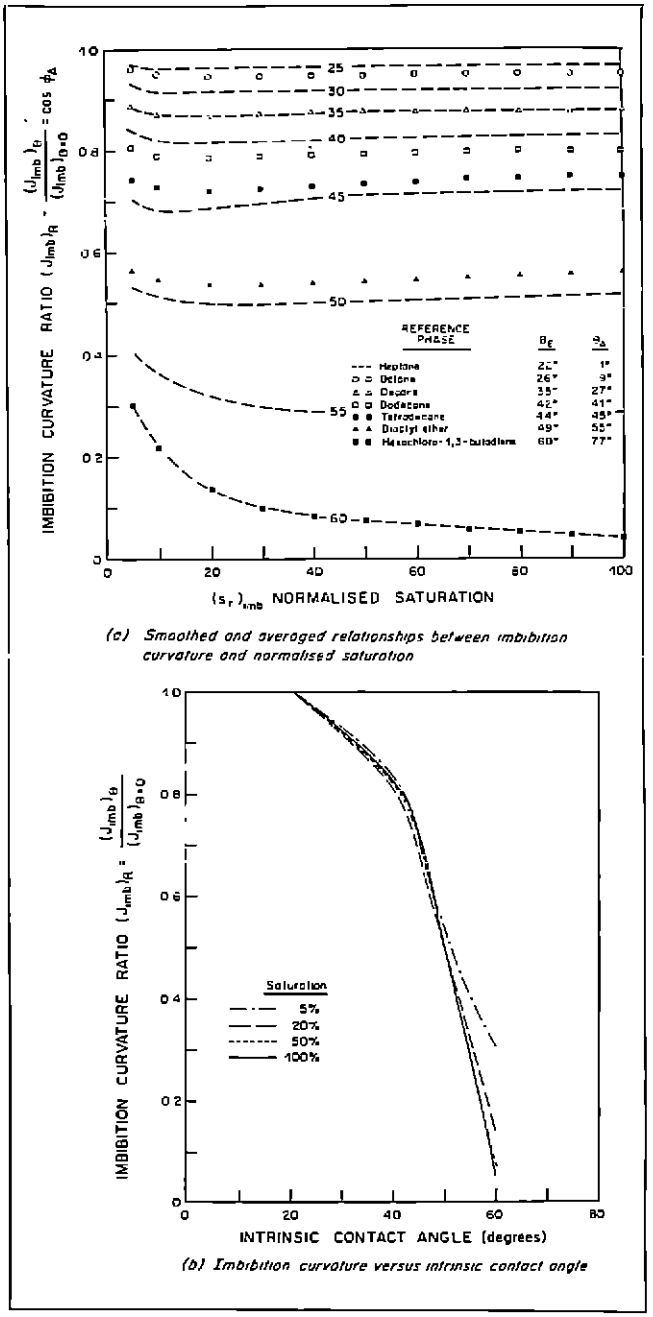


*(a) Smoothed and averaged relationships between imbibition curvature and normalised saturation*

*(b) Imbibition curvature versus intrinsic contact angle*

FIGURE 20 — Imbibition curvature relationships.

After smoothing and averaging results given in Figure 19, data were replotted in Figure 20a. From the position of the averaged data with respect to experimental data, the averaged results correspond to an $\xi$ value of about 0.8. The spread in results provides an indication of the effect of varying $\xi$ in the observed range of 0.55 to 0.89, but differences in pore geometry effects from one core to another may also contribute to this spread.

The smoothed data of Figure 20a were then replotted to obtain a relationship between curvature and contact angle with saturation as parameter (Fig. 20b). The curves shown in Figure 20b were in turn used to obtain the interpolated results, ranging from 25 to 60 degrees at 5-degree intervals, which are included in Figure 20a. Values of curvature ratio above about 50% saturation are probably of greater general reliability because they are less influenced by the dependency of the shape of the imbibition curve on the normalizing saturation, $(s_r^*)_{min}$.

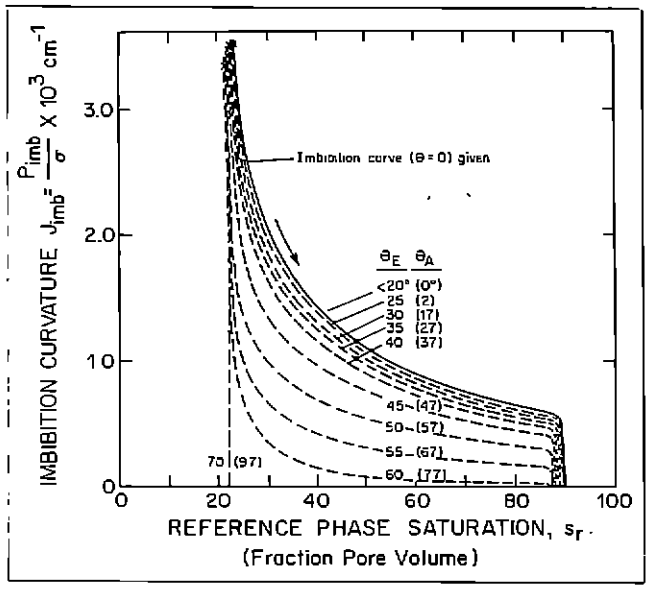


FIGURE 21 — Predicted imbibition data for contact angles of 0 to 60 degrees at 5-degree intervals.

## Prediction of Imbibition Data

As an example of the use of the correlated relationships derived from imbibition data, consider that the imbibition curve for complete wetting is given (Fig. 21) and that curves for 25 to 60 degrees at 5-degree intervals are to be calculated. The complete wetting curve for imbibition begins on the primary drainage curve at an applied capillary pressure corresponding to a curvature, $P_c/\sigma$, of 3.5, and a wetting phase saturation, $(s_r^*)_{min}$, of 23.3%.

Development of the imbibition curve will be considered in detail for a contact angle of 50 degrees, where the value of $(s_r^*)_{min}$ is given by $0.95 \times 23.3 = 22.1\%$. [From Fig. 12d it can be seen that no correction to $(s_r^*)_{min}$ for change in contact angle is required for angles up to about 30°.] The corresponding, externally measured curvature $(P_c/\sigma)$ for the 50-degree system is determined from Figure 13c as $3.5 \times 0.97 \times 10^3$ cm$^{-1}$. Based on the relationship given in Figure 17b, the residual non-wetting phase saturation is predicted to increase from 10% to $1.2 \times 10\% = 12\%$.

The imbibition data for complete wetting is then normalized by substitution in Equation 15.

$$(s_r)_N = \frac{s_r - 23.3}{100 - 23.3 - 10.0} \cdot 100$$

The normalized data are adjusted using the relationships shown in Figure 20a to obtain the relationship between imbibition curvature and normalized saturation for a contact angle of 50 degrees. Next, the normalized saturation values are converted to give the predicted imbibition curve for 50 degrees.

$$s_r = \frac{(s_r)_N (100 - 22.1 - 12)}{100} + 22.1$$

A similar procedure was used to obtain the other predicted imbibition results included in Figure 21.

# Discussion

## GENERAL CLASSES OF UNIFORM-WETTABILITY SYSTEMS AND THEIR INTERRELATIONSHIPS

It is clearly desirable to develop a general account of wetting behaviour which covers the complete con-

tact-angle range from 0 to 180 degrees. In determining the effect of surface roughness on contact angle from capillary rise in tubes[5], receding angles, $\theta_R$, for drainage, and advancing angles, $\theta_A$, for imbibition were measured for liquids with intrinsic angles ranging from 0 to 108 degrees. These were also interpreted as results for intrinsic angles ranging from 72 to 180 degrees simply by redefining the reference phase and interchanging advancing and receding values. The superposition of data in the range of 72 to 108 degrees shown in Figure 3 provides direct confirmation of the validity of this procedure.

The application of this procedure to the capillary pressure data obtained in the present work for porous media is less straightforward. Apparent advancing and receding contact angles[15] for imbibition and drainage respectively are directly related to relative displacement curvatures.

For imbibition,

$$\phi_A = \cos^{-1} (J_{imb})_R \quad \ldots\ldots (16)$$

For drainage,

$$\phi_R = \cos^{-1} (J_{dr})_R \quad \ldots\ldots (17)$$

The presence of residual saturations of either phase can often have a significant influence on displacement curvature. The circumstances under which $\phi_A$ and $\phi_R$ for a system of wettability, $\theta_E$, may be interchanged to give results for a system of wettability $(180° - \theta_E)$ will now be discussed. It will be assumed that model capillary behaviour[10] holds for the systems under discussion. This implies that any change in saturation or fluid distribution due to diffusion of entrapped or hydraulically isolated residual fluid can be neglected.

In giving a general account of the effect of contact angle on displacement, two initial conditions will be considered. The porous media are taken to be initially 100% saturated with either the reference phase (condition R) or the non-reference phase (condition NR). Capillary behaviour for each of the two types of initial condition is related to the other by simple transformations.

For each of these initial conditions, three types of behaviour are identified; these correspond to wetted systems, W, intermediate-wettability systems, I, and non-wetted systems, NW. They are defined by ranges of intrinsic angle, which were selected according to the

TABLE 4 — Classification and Characteristics of Uniformly Wetted Systems

| | Wettability Class | | Wetted (W) | Intermediate (I) | Non-Wetted (NW) |
|---|---|---|---|---|---|
| General Characteristics | Fluid Distribution | | Reference fluid occupies finer pores | Initial fluid remains in finer pores | Non-reference fluid occupies finer pores |
| | Spontaneous Imbibition | | Reference fluid imbibes spontaneously. Rate decreases with increase in $\theta_E$ | No spontaneous imbibition of either phase. | Non-reference fluid imbibes spontaneously. Rate increases with increase in $\theta_E$ |
| | Relative Permeability | | Insensitive to $\theta_E$ | Shifts with $\theta_E$ | Insensitive to $\theta_E$ but distinctly different from wetted systems |
| | Capillary Pressure | | $P_{dr}$ insensitive to $\theta_E$. $P_{imb}$ decreases with increase in $\theta_E$ | $P_{dr}$ and $P_{imb}$ decreases with increase in $\theta_E$ | $P_{dr}$ decreases with increase in contact angle. $P_{imb}$ insensitive to contact angle |
| Initial condition (R) Sr = 100% | Designation | | R, W | R, I | R, NW |
| | Range of Intrinsic Angle $\theta_E$ | | 0° — 62° | 62° — 133° | 133° — 180° |
| | Range of operative contact angle (at rough surface) | Drainage $\theta_R$ | 0° — 10° | 10° — 129° | 129° — 180° |
| | | Imbition $\theta_A$ | 0° — 81° | 81° — 176° | 176° — 180° |
| | Sign of $P_c$ and pore filling sequence | Primary drainage | $+^{ve} P_{dr}$ large-small | $+ P_{dr}$ large-small | $-^{ve} P_{dr}$ small-large |
| | | Imbibition | $+^{ve} P_{imb}$ small-large | $- P_{imb}$ large-small | $-^{ve} P_{imb}$ large-small |
| | Complementary systems | | NR, NW | NR, I | NR, W |
| | Closely related systems | | R, NW RN, W | — | RW NR, NW |
| Initial condition (NR) Sr = 0% | Designation | | NR, W | NR, I | NR, NW |
| | Range of Intrinsic Angle $\theta_E$ | | 0° — 47° | 47° — 118° | 118° — 180° |
| | Range of operative contact angle (at rough surface) | Drainage $\theta_R$ | 0° — 4° | 4° — 99° | 99° — 180° |
| | | Imbibition $\theta_A$ | 0° — 51° | 51° — 170° | 170° — 180° |
| | Sign of $P_c$ and pore filling sequence | Primary imbibition | $+^{ve} P_{imb}$ small-large | $-^{ve} P_{imb}$ large-small | $-^{ve} P_{imb}$ large-small |
| | | Drainage | $+^{ve} P_{dr}$ large-small | $+^{ve} P_{dr}$ large-small | $-^{ve} P_{dr}$ small-large |
| | Complementary systems | | R, NW | R, I | R, W |
| | Closely related systems | | NR, NW R, W | — | NR, W R, NW |

imbibition characteristics given in Table 4. The limiting values of 62 degrees (and 118 degrees) are obtained from the correlated data (Fig. 20b). From the data used to obtain the correlation, it can be seen that these limiting values will vary somewhat from one porous medium to another. The choice of $< 47$ degrees for the limiting case of spontaneous imbibition into a core at $S_{wr} = 100\%$ is based on the observation that for initially dry cores, only one out of six imbibed dioctyl ether ($\theta_E = 49°$), whereas all cores imbibed tetradecane ($\theta_E = 44°$).

The systems were classified as follows. For 100% initial saturation of the reference fluid, condition R, the systems are designated type R,W for $\theta_E$ in the range 0° to < 62°, R,I for 62° to 133° and R,NW for > 133° to 180°. For 100% initial saturation of the non-reference fluid, they are NR,W for the range 0° to < 47°, NR,I for 47° to 118° and NR,NW for > 118° to 180°. The interrelationship of the classes is given in Table 4, together with the sign of drainage and imbibition capillary pressures. The notation L — S or S — L given with the sign of capillary pressure indicates the tendency for larger pores to drain before the smaller or vice versa. For the intermediate-wettability systems R,I and NR,I, the sequence is regarded as anomalous. For drainage, the larger pores tend to drain before the smaller. There is change in sign of capillary pressure for imbibition, with the result that the larger pores will also tend to fill before the smaller. A dominant feature of the intermediate-wettability systems is that neither phase will imbibe spontaneously and the fluid initially saturating the core always remains in the finer pores and associated pendular structures. Because of the effect of this liquid on the over-all mechanism of displacement, behaviour at intermediate-wettability is unique within class R,I or NR,I. Thus, within the class R,I, for example, the results for a system with contact angle $\theta_E$ cannot be used to predict results for (180° — $\theta_E$) or vice versa. Results for R,I at angle $\theta_E$ will, however, be complementary with those for (180° — $\theta_E$) in the class NR,I.

For the intermediate systems, complementary behaviour implies that for

$$(\theta_E)_{R,I} = 180 - (\theta_E)_{NR,I} \quad (18)$$

and a given displacement history,

$$(P_c)_{R,I} = -(P_c)_{NR,I} \quad (19)$$

$$(s_r)_{R,I} = 1 - (s_r)_{NR,I} \quad (20)$$

Thus, values of $\phi_R$ determined experimentally in the present work for class R,I, at an intrinsic angle $\theta_E$, provide values of $\phi_A$ for class NR,I, at an intrinsic angle of (180° — $\theta_E$). Further experimental work involving forced imbibition of liquid into cores containing a residual liquid saturation is needed in order to obtain a more general account of the behaviour of intermediately wet systems.

The behaviour of wetted and non-wetted systems is more self-consistent than that of the intermediately-wet systems, mainly because the wetting liquid occupies the fine pores either initially or after primary drainage or imbibition. For these systems, complementary behaviour between classes, say R,W and NR,NW, implies that for

$$(\theta_E)_{R,W} = 180 - (\theta_E)_{NR,NW} \quad (21)$$

and a given displacement history,

$$(P_c)_{R,W} = -(P_c)_{NR,NW} \quad (22)$$

and

$$(s_r)_{R,W} = 1 - (s_r)_{NR,NW} \quad (23)$$

Complementary behaviour implies that values of $\phi_R$ and $\phi_A$ for class R,W (intrinsic angle range 0° — 62°), for example, can be interchanged to give apparent angles for class NR,NW systems (intrinsic angle range 118° to 180°) and vice versa.

For R,W systems, experimental results show only minor differences in the $\phi_R$ values for primary and secondary drainage. Significant differences are observed for primary and secondary imbibition. However once the wetting phase takes occupancy of the finer pores, then, apart from possible minor differences, subsequent drainage-imbibition cycles will be either the same or complementary to those for the classes described as closely related. This implies that, for these classes, the apparent contact angles $\phi_R$ and $\phi_A$ can be interchanged if the system wettability is redefined as 180° — $\theta_E$.

It may be noted that the frequently used terms wetting and non-wetting phase and the associated definition of capillary pressure have not been used in the present treatment. This is mainly because of the semantic difficulties which would arise and also the problem of determining which phase should be correctly regarded as the wetting phase. In ensuing discussions of water-oil systems, water will always be taken as the reference phase. For reservoir systems and most displacement experiments performed in the laboratory in connection with oil recovery, the initial condition is 100% saturation of the reference phase. For liquid-gas systems, the liquid is taken as the reference phase, as is the case in the present study.

## CLASSIFICATION OF RESERVOIR WETTABILITY

Treiber *et al.* somewhat arbitrarily chose water advancing contact angles in the ranges 0° to 75°, 75° to 105°, and 105° to 180° to classify reservoirs as respectively water-wet, intermediately-wet or oil-wet[2]. In the classification scheme given in Table 4, the water-wet group should correspond to advancing angles of 0° to 62° at a smooth surface. The intermediately-wet group would range from the water-advancing angle of 62° up to a water-receding angle of about 133°, at which condition oil should spontaneously displace water. If the aforementioned classes are redefined with respect to advancing contact angles of 0° to 62°, 62° to 133° and 133° to 180°, there is a large increase in the number of intermediately-wet reservoirs (see Table 5). Except for one case, this increase is entirely at the expense of the number of reservoirs which were classified as oil-wet.

In practice, large contact-angle hysteresis is generally observed for reservoir fluids at smooth mineral surfaces. Since a water-receding angle of 133° should be used to distinguish between intermediate and oil wetness, the number of systems of intermediate wettability is even higher. For example, if the advancing angle corresponding to a receding angle of 133° were only 10° higher, an additional 11 of the 55 studied reservoirs would be classified as intermediately-wet, leaving only 4 in the oil-wet category; if the hysteresis were 20°, only one of the reservoirs would be oil-wet (see Table 5).

This reclassification according to spontaneous imbibition behaviour would also appear to be consistent with an undocumented comment by Craig that most reservoirs are believed to have intermediate-wettability, with no strong preference for either oil or

TABLE 5 — Distribution of water-wet, intermediately-wet and oil-wet reservoirs based on advancing contact-angle measurements on smooth mineral surfaces for fluids from 55 reservoirs

| Wettability Class | Water-Wet | Intermediate | Oil-wet |
|---|---|---|---|
| Defining contact angle range used by Treiber *et al.* [2] ($\theta_A$ at smooth mineral surface) | 0° — 75° | 75° — 105° | 105° — 180° |
| No. of Sandstone Reservoirs | 13 (43%) | 2 (7%) | 15 (50%) |
| No. of Carbonate Reservoirs | 2 (8%) | 2 (8%) | 21 (84%) |
| TOTAL: | 15 (27%) | 4 (7%) | 36 (66%) |
| Defining contact angle range from classification used in present work | $\theta_A < 62°$ | $\theta_A > 62°$ $\theta_R < 133°$ | $\theta_R > 133°$ ($\theta_R = \theta_A$) |
| No. of Sandstone Reservoirs | 12 (40%) | 10 (33%) | 8 (27%) |
| No. of Carbonate Reservoirs | 2 (8%) | 16 (64%) | 7 (28%) |
| TOTAL: | 14 (26%) | 26 (47%) | 15 (27%) |
| Defining contact angle range | as above | as above | $\theta_R > 133°$ ($\theta_R = \theta_A - 10°$) |
| TOTAL: | 14 (26%) | 37 (67%) | 4 (7%) |
| Defining contact angle range | as above | as above | $\theta_R > 133°$ ($\theta_R = \theta_A - 20°$) |
| TOTAL: | 14 (26%) | 40 (73%) | 1 (2%) |

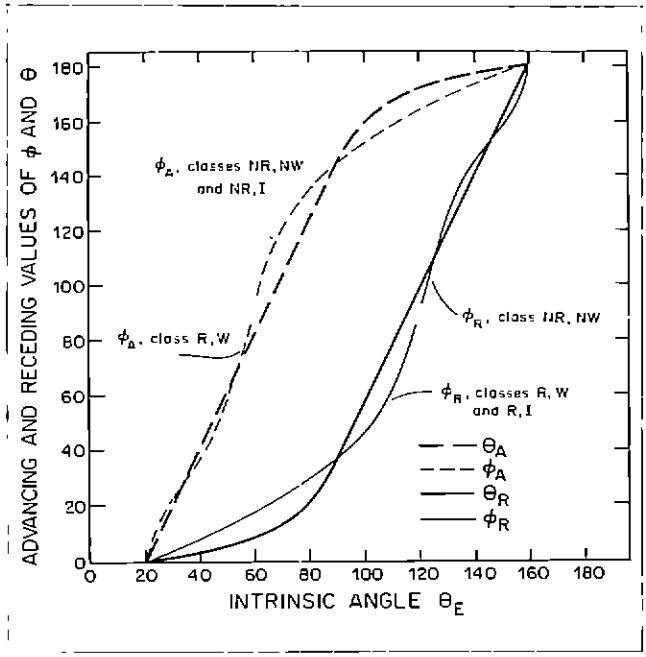


FIGURE 22 — Comparison of advancing and receding contact angles ($\theta_A$ and $\theta_R$) measured at rough surfaces with apparent advancing and receding contact angles ($\phi_A$ and $\phi_R$) obtained from capillary pressure correlations.

water[18]. The presence of connate water in the finer pores, even at relatively high values of advancing contact angle, may be of special significance to oil recovery mechanisms of the type suggested by Salathiel[17]. Also, it should be noted that a mixed wettability condition of the type envisaged by Salathiel is not a necessary condition for retention of water in the finer pores.

## THE ROLE OF PORE GEOMETRY IN DETERMINING DISPLACEMENT CURVATURES

Consideration will now be given to the magnitude of apparent contact angles with regard to determining the relative influence of pore geometry and contact angle on displacement curvatures. Because results for a given contact angle could be correlated reasonably well from one core to another, it follows that the role of pore geometry, whatever it may be, is reasonably consistent for the cores which were studied.

The scatter in the results presented in Figures 13a and 19 provide an indication of the differences due to pore geometry. However, the method of correlation will also contribute to this scatter to some extent; in the case of imbibition, for a given contact angle, the degree of desaturation may make a major contribution to the observed range of results. In using the correlations which have been developed, judgment should, of course, always be exercised with regard to the data from which the correlations were derived.

### Operative Contact Angles

For the porous media, receding angles will be operative during drainage and advancing angles during imbibition. Because these angles cannot be measured directly, it will be assumed that the angles $\theta_R$ and $\theta_A$ shown as functions of $\theta_E$ in Figure 3 are the operative contact angles for the porous media which have been studied. With this assumption, the relative contribution of pore geometry can be assessed by comparing operative contact angles $\theta_R$ and $\theta_A$ with apparent contact angles $\phi_R$ and $\phi_A$.

### Comparison of Operative Contact Angles with Apparent Contact Angles

At a given wettability, the $\phi$ values are dependent on class of system and its history, saturation and choice of normalizing procedure. Values of $\phi_R$ were taken from Figure 13c and values of $\phi_A$ from Figure 20a at 100% saturation in both cases, and are seen to be fairly constant down to saturations of about 40%.

Plots of apparent contact angles $\phi_A$ and $\phi_R$ versus intrinsic angle $\theta_E$ are shown in Figure 22 together with the smoothed values of $\theta_R$ and $\theta_A$ taken from Figure 3. The apparent contact angle data were extended by redefining the intrinsic angle as $(180 - \theta_E)$ and interchanging $\phi_R$ and $\phi_A$. The classes of system (see Table 4) to which the $\phi$ values apply are indicated in Figure 22.

A remarkable feature of these results is the close correspondence between apparent contact angles ($\phi_R$ and $\phi_A$) and the angles observed at rough surfaces ($\theta_R$ and $\theta_A$). Whereas the $\theta$ values were derived from displacement pressures in roughened cylindrical tubes, the $\phi$ values were determined from displacement pressures in porous media of highly complex geometry. Departure from cylindrical pore geometry appears to have only minor effect on the manner in which contact angle and pore geometry interact to determine dis-

placement curvatures in the porous media which have been studied. Because of the close agreement between $\phi_R$ and $\theta_R$ and between $\phi_A$ and $\theta_A$, it follows that change in displacement curvature due to wettability is approximately proportional to the cosine of the operative contact angle.

This conclusion was somewhat unexpected. The results would appear to support use of the capillary tube model to predict the effect of contact angle on displacement curvature. Several authors have pointed out that the tube model is a highly unrealistic representation of the geometry of porous material in general. Displacement pressures calculated for doughnuts[18, 19], parallel spaced rods[20], cones[21, 22] and sphere packings[23] all demonstrate a marked interaction of pore geometry and contact angle in determining displacement curvature. Such calculations suggest that significant geometric effects would probably be operative in actual porous media.

The close agreement between $\theta_A$ and $\phi_A$ for cores containing an initial reference phase saturation should probably be regarded as somewhat fortuitous. As previously noted, there was a tendency for $\phi_A$ to increase with degree of desaturation, $\xi$, but this was not severe. This point is illustrated by the scanning curves shown in Figure 10 for imbibition of dioctyl ether into core No. 4. For this system, $\theta_E$ is 49° and, from Figure 20, $\theta_A$ and $\phi_A$ are 57° and 54° respectively. Significant pore geometry effects do appear to come into play for imbibition into a dry core, as evidenced by the observation that dioctyl ether ($\theta_A = 57°$) would not spontaneously imbibe ($\phi_A > 90°$) into the same core when it was initially dry. However imbibition into a dry core is of less relevance to reservoir rocks, because there is generally a significant connate water saturation which occupies the finer pore spaces.

## Curvature Correction Factors

A theoretical study of the effect of contact angle on displacement curvature in sphere packings is reported by Melrose[23]. The effect of contact angle on capillary-pressure hysteresis was determined in the absence of contact-angle hysteresis. The effect of pore geometry was expressed as a curvature correction factor Z, where

$$\cos\phi = Z\cos\theta \qquad (24)$$

$\phi$ being the apparent contact angle and $\theta$ the operative angle. For drainage, Z, was slightly greater than unity over the contact-angle range for which it was determined. For this range, it is seen from Figure 23a that the model calculations are in fairly satisfactory agreement with those determined from the present work where $Z_{dr}$ is defined by

$$\cos\phi_R = Z_{dr}\cos\theta_R \qquad (25)$$

The values of $Z_{imb}$ determined from

$$\cos\phi_A = Z_{imb}\cos\theta_A \qquad (26)$$

were also close to unity. In contrast, those calculated for sphere packings[23] showed a marked decrease with increase in contact angle which depended on both packing array and initial saturation (Fig. 23a).

Experimentally, it has been observed that imbibition rates for a system of given wettability were significantly lower for an initially dry system[4]. This is consistent with model calculations for both invasion into a pore formed by two stacked doughnuts[19] and for pores formed by packed spheres[23]. Three conditions were considered for the sphere packing: (a) no pendular rings; (b) pendular rings at the pressure of drainage; (c) equilibrium behaviour with pendular rings at the pressure of imbibition. The physical significance of these three states is discussed by Melrose[23]. (Indirect measurements of pendular ring pressures for a drained sphere packing at irreducible saturation suggests the second condition may be the most realistic for a previously drained system[24].) The three conditions, as listed, correspond to increasing values of initial liquid saturation. Curvature correction factors for these three conditions fall below unity and, as can be seen from Figure 23a, their relative magnitudes for a given wettability increase according to the sequence of conditions (b), (c), (a). However, these corrections are not sufficient to cause departure from the general observation that displacement curvatures at which imbibition occurs tend to increase

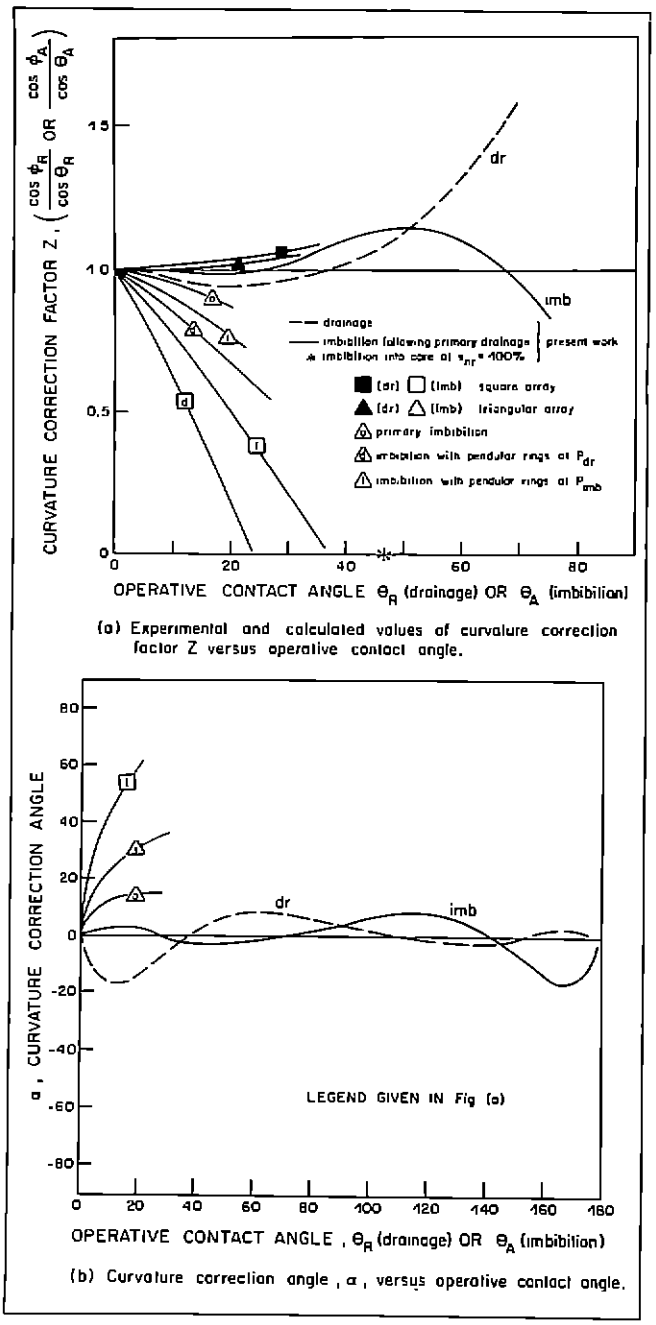


FIGURE 23 — Curvature corrections for pore geometry effects.

with initial saturation, provided, of course, that the initial saturation is essentially immobile.

An alternative method of presenting a correction factor for the effect of pore geometry is suggested by pore models such as that shown in Figure 2e. Results can be interpreted in terms of a curvature correction angle, $\alpha$, which is added to the operative contact angle. Thus,

$$\cos \phi_R = \cos (\theta_R + \alpha_{dr}) \quad (27)$$

and

$$\cos \phi_A = \cos (\theta_A + \alpha_{imb}) \quad (28)$$

Values of $\alpha_{dr}$ and $\alpha_{imb}$ derived from Figure 23a are plotted against intrinsic contact angle in Figure 23b. This approach has the advantage that the correction is related to a relatively simple model and problems associated with the discontinuity in Z values at $\theta = 90°$ do not arise.

The differences in the curvature correction terms calculated for imbibition into sphere packings and those determined in the present work (see Fig. 23a or b) serve to point out the possible importance of pore geometry effects for different types of porous media. However, electron micrographs of consolidated porous rock[25, 26] and the PTFE cores used in the present work[4, 9] show both types of media to be broadly similar with regard to randomness in appearance, especially in the sense of being clearly distinguishable from sphere packings and other regular arrangements. This observation coupled with the general consistency in behaviour of the six cores studied is encouraging with regard to the general validity of the correlations which have been presented.

## RESERVOIR WETTABILITY AND IMPROVED RECOVERY

### Mobilization of Residual Oil

Considerable attention is now being given to enhanced recovery through low-interfacial-tension flooding. Residual oil in a flooded-out water-wet region is held as discrete capillary structures known as ganglia, and each ganglion may occupy one or more pores. The basic principle of the low-interfacial-tension flood is to first mobilize residual oil by decreasing the interfacial tension to a level where the ratio of viscous to capillary forces is sufficient to displace the entrapped oil[27].

Melrose and Brandner recently presented a review and development of investigations concerned with the requirements for mobilization of residual oil[28]. Displacement of a ganglion involves drainage at its leading edge and imbibition at the trailing edge. The capillary force, $\triangle P_c$, which must be overcome is given by

$$\triangle P_c = P_{dr} - P_{imb} \quad (29)$$

or

$$\triangle P_c = \sigma_{ow} (J_{dr} - J_{imb}) \quad (30)$$

where $\sigma_{ow}$ is the oil-water interfacial tension. This concept was incorporated into a method for estimating the conditions required for displacement of residual oil; calculated results were consistent with those observed experimentally under strongly water-wet conditions.

Melrose and Brandner also considered the effect of wettability on the magnitude of the capillary forces which resist displacement. Using the values of $J_{dr}$ and $J_{imb}$ determined from model calculations for spheres, it was concluded that complete water wetting is the optimum condition for displacement. For a sphere packing assumed to have a contact angle of 45°, operative for both drainage and imbibition, the capillary forces resisting displacement of oil ganglia were estimated to be almost doubled.

Consideration of the results of the present work leads to a qualitatively similar conclusion, but for somewhat different basic reasons. The differences in drainage and imbibition capillary pressures observed in the present work now appear to be due mainly to contact-angle hysteresis caused by microscopic surface roughness rather than to larger-scale effects of pore geometry.

In selecting the drainage and imbibition pressures which pertain to the displacement of ganglia, some judgment is needed, because capillary pressures of drainage and imbibition are both functions of saturation. For imbibition, the curvature corresponding to residual saturation shown in Figure 11 as $J^*_{imb}$ was chosen; a low value of imbibition curvature was taken, because Raimondi and Torcaso have shown that entrapment of residual oil occurred very close to the final stages of imbibition[29]. The drainage curvature $J^*_{dr}$ was taken to be $J_E$, as determined from the drainage curvature at 100% saturation (Fig. 11). This value of $J^*_{dr}$ is associated with the largest pores, which tend to drain first and are also the pores in which residual oil will tend to be entrapped. The choice of $J^*_{dr}$ and $J^*_{imb}$ values is obviously arbitrary to some extent. The main reason for this specific choice of values is that they both correspond to 100% normalized saturation in Figures 13c and 20a for all cores at all contact angles. From the values shown in Figures 13c and 20a, it can be seen that the change in curvature ratio at a given contact angle is reasonably independent of saturation for both drainage and imbibition down to normalized saturations of about 50%.

Following Melrose and Brandner[28], the effect of wettability on the magnitude of the forces required to displace residual oil will be expressed as $W(\theta)$, the ratio of the displacing force at contact angle $\theta$ to that when the contact angle is zero.

$$W(\theta) = \frac{J^*_{dr(\theta)} - J^*_{imb(\theta)}}{J^*_{dr(\theta=0)} - J^*_{imb(\theta=0)}} \quad (31)$$

Writing

$$\frac{J^*_{dr(\theta)}}{J^*_{dr(\theta=)0}} \text{ as } (J_R)_{dr}$$

and

$$\frac{J^*_{imb(\theta)}}{J^*_{imb(\theta=0)}} \text{ as } (J_R)_{imb}$$

and

$$\frac{J^*_{imb}}{J^*_{dr}} \text{ as } J^*$$

we have

$$W(\theta) = \frac{1}{(1 - J^*)} (J_R)_{dr} - \frac{J^*}{(1 - J^*)} (J_R)_{imb} \quad (32)$$

Values of J* were determined for all cores. The average value was 0.645, and the maximum and minimum values were .675 and .625 respectively. These values were used to obtain relationships between $W(\theta)$ and $\theta_E$, shown in Figure 24. It is seen that in the intermediate contact angle range, the model calculations predict the capillary forces for retention of oil to be

almost quadrupled with respect to those for complete wetting. Values of $W(\theta)$ are also shown in Figure 24 for displacement of a fluid slug from roughened tubes with $J^*$ of 0.645. The close correspondence between these values and those for the porous media serves to illustrate that variation in $W(\theta)$ for the latter is mainly due to contact-angle hysteresis, rather than pore geometry. Nevertheless, the conclusion reached by Melrose and Brandner that strong water wetting is the optimum condition for low-interfacial-tension flooding is supported by the present work.

It is sometimes assumed that capillary forces which resist displacement are proportional to the cosine of the contact angle and are therefore minimized when the contact angle is 90°. Values of $W(\theta)$ calculated from this assumption with an assumed ratio of imbibition to drainage pressures of 0.645 are included in Figure 24. The distinct differences in the estimated values of $W(\theta)$ indicate the need to take contact-angle hysteresis into account when considering the effects of wettability on displacement of residual oil.

It should be noted that values of $W(\theta)$ estimated for porous media are based on a model where residual oil is assumed to be held as ganglia of a form which are subject to viscous drag forces that are equivalent to those trapped in strongly water-wet systems. However, it is likely that there are important differences in capillary structure which could cause change in flow mechanism with contact angle. In some circumstances, continuity of the oil phase may not be lost completely[17].

As an extreme example, when the value of $W(\theta)$ for porous media falls to unity at high intrinsic contact angles, the non-reference phase will occupy the finer pores. This corresponds to a strongly oil-wet condition, which would be highly unfavourable to mobilization of oil by viscous forces through low-tension flooding. Studies on a water-wet rock of the effect of pressure drop and coring on displacement of laboratory-established connate water or residual oil saturations[30, 31] serve to illustrate this point. After establishing a given condition, abnormally high pressure gradients were applied to the flowing phase. At 1000 psi/ft, the residual oil was reduced by 18%, whereas no connate water was produced by flowing oil in the same core at this pressure gradient. At 2000 psi/ft, the residual oil had been reduced by 38% and the connate water by only 4%.

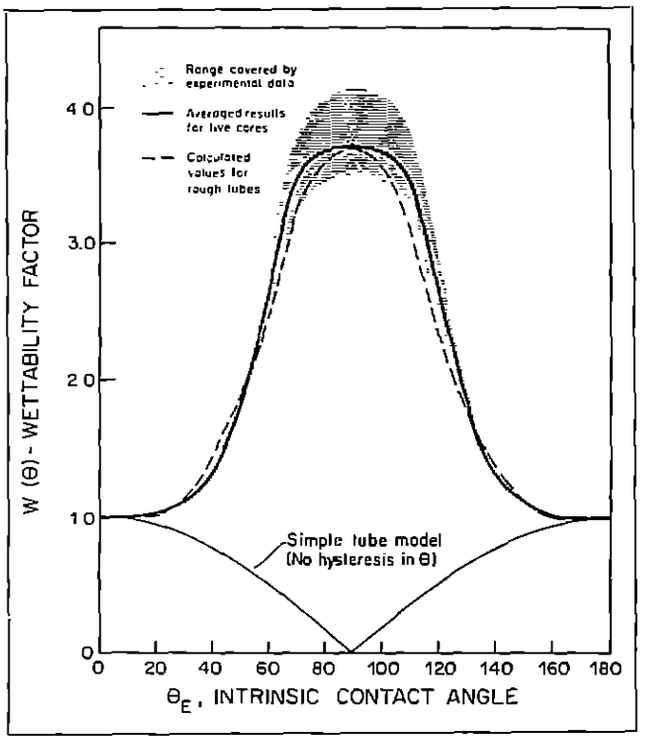


FIGURE 24 — Relationships between wettability factor for displacement of residual non-reference phase and $\theta_E$ for tubes and porous media.

## Reservoir Wettability and Wettability Alteration

Although the present work is concerned with systems of uniform wettability, it is not, of course, assumed that this type of wettability holds for reservoirs in general. Because wettability is determined by the interaction of rock and fluid properties, a possible alternative approach to obtaining wettability control is through the use of various crude oils and rock minerals chosen according to the angle which they exhibit. Although suitable crudes are believed to exist, the disadvantage of not being able to properly specify the system is a drawback with respect to developing a reproducible body of knowledge on wetting behavior. However, work of this type would be a logical extension of the present work.

The nature and causes of reservoir wettability remain an open question. Departure from uniform wettability may arise because of mixed minerological composition[32], fluid distribution[17] or other factors. If mixed wettability conditions do have an important influence on displacement characteristics, this will show up as departures from the general pattern of behaviour which has been determined for uniformly wetted systems. For example, field engineers have sometimes observed that a core initially saturated with water will imbibe oil, whereas the same core initially saturated with oil will imbibe water. Such behaviour is at odds with that expected of a system having uniform wettability.

With regard to the problem of treating reservoir wettability as a quantitatively engineering parameter, it is recommended that uniform wettability be assumed unless there are facts which suggest otherwise. In terms of engineering accuracy, this is considered to be an advance on the often-made, but less likely, assumption that most reservoirs are strongly water-wet.

It may be noted that in order to observe spreading of hydrocarbons against water on mineral surfaces, extreme care is needed in preparing a clean solid surface and obtaining pure hydrocarbon liquids. In the presence of trace amounts of polar impurities which adsorb on the solid surface, finite contact angles will generally be observed. For example, Owens and Archer report a contact angle of 46° for water against a refined hydrocarbon[33]. Because of the wide variety of compounds present in crude oil, it seems unlikely that the often claimed condition of complete wetting (i.e., the spreading condition) actually prevails in any oil reservoir. In fact, for those reservoirs where water will spontaneously imbibe, it seems more likely that the wetting conditions correspond to systems with intrinsic angles in the range of 30° to 60°. Angles in this range were also commonly found in a wettability study of low-molecular-weight surfactants known to occur in crude oil[7]. It may also be noted that, within this range, residual saturations were observed to increase with contact angle (Fig. 17), capillary pressures are extremely sensitive to contact angle in the range of 45° to 60° (Fig. 21), and imbibition

rates can be expected to increase by more than an order of magnitude when a system is changed from weakly to strongly water-wet.

The significance of production rate to economic recovery of petroleum has recently been the focus of considerable attention in Alberta[34]. It would appear from the foregoing discussion that enhanced recovery might result from relatively minor adjustments in wettability toward increased water wetness. Measurement of wettability shift in water-wet systems should not present any great difficulties, as they will be indicated by both imbibition capillary pressures and imbibition rates. As an example of how the desired change might be achieved, it may be noted that Bobek *et al.* reported that addition of lime to water used in imbibition tests resulted in increased imbibition rate[35].

A distinctly different possibility for high waterflood recoveries by wettability adjustment may lie in factors related to the abnormally low residual oil saturations which are sometimes achieved by waterflooding. A notable example is the East Texas field. Richardson *et al.* showed that low residuals could also be obtained in the laboratory for preserved East Texas cores by subjecting them to prolonged waterflooding[35]. When displacement tests were conducted on the same cores, rendered strongly water-wet by extraction, distinct cut-off of oil production and much higher residuals were obtained. The preserved cores were reported to spontaneously imbibe water. Thus, according to this imbibition behaviour, the preserved cores, although not strongly water-wet, would appear to be related to R,W-type wettability (Table 4).

The low residuals were later ascribed to a gravity-assisted flow mechanism involving a particular type of mixed wettability condition[17] which maintains paths for continuous flow of oil. The wettabiilty condition of the East Texas preserved cores was believed to have been reproduced by contacting initially water-wet cores with a mixture of East Texas crude oil and heptane. When this mixture was contacted against a clean silica surface under water, it was observed to deposit a strongly oil-wetting film on the solid in the region of contact. When the mixture was used to displace water from an initially strongly water-wet core, it was concluded that a mixed wettability condition was induced; the rock contacted with the oil became strongly oil-wet, while that overlain by retained water remained water-wet. Since the wettability of the drained rock surfaces may be expected to dominate subsequent displacement behaviour, such a system would probably exhibit some of the characteristics of the wettability type R.NW (see Table 4). No spontaneous imbibition measurements were reported for the induced wettability cores.

Although there may be some basic differences between the preserved and induced wettability systems, the most important feature of both types was that low residuals could be achieved by prolonged waterflooding. Reports of comparably low residuals in other fields suggest that the flow mechanism envisaged by Salathiel may not be peculiar to the East Texas field alone.

## EVALUATION OF RESERVOIR WETTABILITY

At present there is a paucity of definitive knowledge concerning the wetting behaviour of reservoirs. For larger reservoirs where wettability may be of concern, laboratory tests are run at conditions which are designed to duplicate those of the reservoir. Reservoir-condition tests are very costly to perform and methods of checking their validity are limited.

Unfortunately, there does not appear to be an instance where a comprehensive set of reservoir-condition tests have been backed up by data which would permit results to be directly compared with the behaviour which has been found for uniformly wetted systems. Sets of relative permeability, capillary pressure and imbibition data run at both reservoir conditions and at complete wetting, together with contact-angle data for reservoir fluids, are needed. From the general form of results, it should be possible to assess how well uniform wettability serves as a model for a given reservoir system. Even in cases where wetting behaviour is obviously more complex, knowledge of the behaviour of uniformly wetted systems[6] will still be of value as an interpretative guide.

## Summary


1. In controlled wettability studies involving six types of *PTFE* porous media, it was found that capillary displacement curvatures changed systematically with intrinsic contact angles measured as smooth surfaces. This showed that the effect of surface roughness on contact angle and the interaction of contact angle and pore geometry to determine displacement curvatures was reasonably consistent from one core to the next.

2. Results could be correlated to give general relationships for the effect of contact angle on capillary pressure for uniformly wetted systems.

3. Drainage curvatures were fairly insensitive to intrinsic contact angle until values greater than about 73 degrees were reached. Imbibition curvatures were highly sensitive to intrinsic contact angles in the range of 30 degrees to 62 degrees, which is the estimated upper limit for spontaneous imbibition.

4. Retained reference-phase (liquid) saturations were found to decrease with increase in contact angle. Residual non-reference-phase (gas) saturations tended to increase with contact angle.

5. Changes in drainage and imbibition capillary pressure were approximately proportional, respectively, to the cosines of the receding and advancing contact angles observed at roughened surfaces.

6. Solid-fluid interactions and the effects of surface roughness on contact angle are of primary importance in determining capillary displacement curvatures; the influence of geometric effects due to pore shape is secondary.

7. System wettability can be classified as wetted, intermediate or non-wetted according to imbibition behaviour.

8. Available contact-angle data indicate that a significant proportion of reservoirs are of intermediate wettability. Strongly oil-wet reservoirs in which oil displaces connate water from the finer pores of a rock are probably rare.

9. Results suggest that improved recovery and increased rates of recovery could result from a small reduction in contact angle for systems which are weakly water-wet.

10. Model calculations for ganglia indicate that complete or strongly water-wet conditions are most favourable for mobilization of discontinuous residual oil by low-interfacial-tension flooding.

## Acknowledgment

The author gratefully acknowledges the assistance of Yoshiaki Ito.

## Nomenclature

### English

| | |
|---|---|
| $P_c$, P | = capillary pressure |
| s | = saturation |
| $s_{rI}$ | = irreducible reference phase saturation |
| $s^*$ | = normalizing saturation |
| r | = radius or characteristic pore dimension |
| J | = mean curvature |
| Z | = curvature correction factor |
| W(θ) | = wettability factor for displacement of residual oil |
| $(s_r^*)_{min}$ | = reference phase saturation prior to imbibition |
| $(s_r^*)_\infty$ | = estimated reference phase saturation at infinite applied capillary pressure] |
| $R_rW$ $R_rI$ $R_rNW$<br>$NR_rW$ $NR_rI$ $NR_rNW$ | = classes of wettability defined in Table 4 |

### Greek

| | |
|---|---|
| α | = curvature correction angle |
| θ | = contact angle |
| σ | = interfacial tension |
| ϕ | = apparent contact angle |
| ξ | = degree of desaturation |

### Frequently used subscripts

| | |
|---|---|
| A | = advancing |
| E | = intrinsic with θ, entry value with J or P |
| dr | = drainage (increasing reference phase) |
| imb | = imbibition (decreasing reference phase) |
| r | = reference phase |
| nr | = non-reference phase |
| N | = normalized |
| Ni | = normalized with respect to $s_{ri}$ |
| R | = receding with θ or ϕ, otherwise ratio |

## References

(1) Wagner, O. R., and Leach, R. O.: Improving Oil Displacement Efficiency by Wettability Adjustment. Trans., AIME, *216*, 65 (1959).

(2) Treiber, L. E., Archer, D. L., and Owens, W. W.: Laboratory Evaluation of the Wettability of Fifty-Five Oil Producing Reservoirs. Soc. Petr. Eng. J., *12*, 531 (1972).

(3) McCaffery, F. G., and Bennion D. W.: The Effect of Wettability on Two-Phase Relative Permeabilities. J. Can. Pet. Tech., *13*, 42 (1974).

(4) McCaffery, F. G., and Bennion, D. W.: Experimental Study of the Relationship of Contact Angles to Imbibition in Porous Media. Reprint, 48th National Colloid Symposium, Austin, Texas, June 1974, p. 124.

(5) Morrow, N. R.: The Effects of Surface Roughness on Contact Angle with Special Reference to Petroleum Recovery. J. Can. Pet. Tech., *14*, 42 (1974).

(6) Morrow, N. R., and McCaffery, F. G.: Displacement Studies in Uniformly Wetted Porous Media. Society of Chemical Industry International Symposium on 'Wetting', Loughborough, England, September 1976 (in press).

(7) Morrow, N. R., Cram, P. J., and McCaffery, F. G.: Displacement Studies in Dolomite with Wettability Control by Octanoic Acid. Soc. Petr. Eng. J., *13*, 221 (1973).

(8) Fox, H. W., and Zisman, W. A.: The Spreading of Liquids on Low Energy Surfaces. I. Polytetrafluoroethylene, J. Colloid Interface Sci., *5*, 514 (1950).

(9) Morrow, N. R., and Mungan, N.: Mouillabilité et Capillarité en Milieux Poreux. Revue IFP, *26*, 629 (1971).

(10) Morrow, N. R., and Harris, C. C.: Capillary Equilibrium in Porous Materials. Soc. Petr. Eng. J., *5*, 15 (1965).

(11) Morrow, N. R.: Physics and Thermodynamics of Immiscible Displacement in Porous Media. Ind. Eng. Chem., *62*, 32 (1970).

(12) Morrow, N. R.: Irreducible Wetting Phase Saturations in Porous Media. Chem. Eng. Sci., *25*, 1799 (1971).

(13) Morrow, N. R.: Small Scale Packing Heterogeneities in Porous Sedimentary Rocks. Bull. A.A.P.G., *55*, 514 (1971).

(14) Thomeer, J. H. M.: Introduction of a Pore Geometrical Factor Defined by the Capillary Pressure Curve. J. Pet. Tech., 73 (March 1960).

(15) Harris, C. C., Jowett, A., and Morrow, N. R.: Effect of Contact Angle on the Capillary Properties of Porous Masses. Trans. Inst. Min. Metall., *73*, 335 (1963-64).

(16) Craig, F. F., Jr.: *The Reservoir Engineering Aspects of Waterflooding*. Monograph Series *3*, Society of Petroleum Engineers of AIME, Dallas 1971.

(17) Salathiel, R. A.: Oil Recovery by Surface Film Drainage in Mixed-Wettability Rocks. J. Pet. Tech., *25*, 1216 (1973).

(18) Purcell, W. R.: Interpretation of Capillary Pressure Data. Trans., AIME, *189*, 369 (1950).

(19) Jones-Parra, J.: Comments on Capillary Equilibrium. Trans., AIME, *198*, 314 (1953).

(20) Cassie, A., and Baxter, S.: Wettability of Porous Surfaces. Trans. Faraday Soc., *40*, 546 (1944).

(21) McCardell, W. M.: A Review of the Physical Basis for the Use of the j-Function. Pet. Res. Comm., Texas A & M College, 1955.

(22) Philip, J. R.: Limitations on Scaling by Contact Angle. Soil Sci. Soc. Amer. Proc., *35*, 507 (1971).

(23) Melrose, J. C.: Wettability as Related to Capillary Action in Porous Media. Soc. Petr. Eng. J., 259 (September 1965).

(24) Harris, C. C., and Morrow, N. R.: Pendular Moisture in Packings of Equal Spheres. Nature, *203*, 706 (1964).

(25) Weinbrandt, R. M., and Fatt, I.: A Scanning Electron Microscope Study of the Pore Structure of Sandstone. J. Petr. Tech., *21*, 543 (1969).

(26) Farley, J. R., Miller, B. M., and Schoettle, V.: Design Criteria for Matrix Stimulation with Hydrochloric-Hydrofluoric Acid. J. Petr. Tech., *22*, 433 (1970).

(27) Taber, J. J.: Dynamic and Static Forces Required to Remove a Discontinuous Oil Phase from Porous Media Containing Both Oil and Water. Soc. Petr. Eng. J., *9*, 3 (1969).

(28) Melrose, J. C., and Brandner, C. F.: Role of Capillary Forces in Determining Microscopic Displacement Efficiency for Oil Recovery by Waterflooding. J. Can. Pet. Tech., *13*, 54 (1974).

(29) Raimondi, P., and Torcaso, M. A.: Distribution of the Oil Phase Obtained Upon Imbibition of Water. Soc. Petr. Eng. J., 49 (March 1964).

(30) Jenks, L. H., Huppler, J. D., Morrow, N. R., and Salathiel, R. A.: Fluid Flow Within a Porous Medium Near a Diamond Core Bit. J. Can. Petr. Tech., *7*, 172 (1968).

(31) Jenks, L. H., Huppler, J. D., Morrow, N. R., and Salathiel, R. A.: Coring for Reservoir Connate Water Saturations. J. Petr. Tech., 21, 932 (1969).

(32) Fatt, I., and Klikoff, W. A., Jr.: Effect of Fractional Wettability on Multiphase Flow Through Porous Media. Trans., AIME, *216*, 426 (1959).

(33) Owens, W. W., and Archer, D. L.: The Effect of Rock Wettability on Oil-Water Relative Permeability Relationships. J. Petr. Tech., 873 (July 1971).

(34) The Sensitivity of Crude Oil Recovery to Production Rate and the Need for Surveillance of the Effect of Production Rate on Recovery and for Regulation of Production Rate. Energy Resources Conservation Board, Calgary, Alberta, 1975.

(35) Bobek, J. E., Mattax, C. C., and Denekas, M. O.: Reservoir Rock Wettability — Its Significance and Evaluation. Trans. AIME, *213*, 155 (1958).

(36) Richardson, J. G., Perkins, F. M., Jr., and Osoba, J. S.: Differences in Behavior of Fresh and Aged East Texas Woodbine Cores, Trans., AIME, *204*, 86 (1955).